Ca^{2+} Influx Pathways Mediated by Swelling or Stores Depletion in Mouse Thymocytes

PAUL E. ROSS and MICHAEL D. CAHALAN

From the Department of Physiology and Biophysics, University of California, Irvine, California 92717

ABSTRACT We used fura-2 video imaging to characterize two Ca^{2+} influx pathways in mouse thymocytes. Most thymocytes (77%) superfused with hypoosmotic media (60% of isoosmotic) exhibited a sharp, transient rise in the concentration of intracellular free Ca^{2+} ($[Ca^{2+}]_i$). After a delay of ≈70 s, these swelling-activated $[Ca^{2+}]_i$ (SWAC) transients reached ≈650 nM from resting levels of ≈100 nM and declined with a time constant of 20 s. Peak $[Ca^{2+}]_i$ during transients correlated with maximum volume during swelling. Regulatory volume decrease (RVD) was enhanced in thymocytes exhibiting SWAC transients. Three lines of evidence indicate that Ca^{2+} influx, and not the release of Ca^{2+} from intracellular stores, underlies SWAC transients in thymocytes. First, thymocytes swollen in Ca^{2+}-free media failed to respond. Second, Gd^{3+} and La^{3+} inhibited SWAC influx with K_d's of 3.8 and 2.4 μM, respectively. Finally, the depletion of Ca^{2+} stores with thapsigargin (TG) before swelling did not inhibit the generation, nor decrease the amplitude, of SWAC transients. Cell phenotyping demonstrated that SWAC transients are primarily associated with immature $CD4^-CD8^-$ and $CD4^+CD8^+$ thymocytes. Mature peripheral lymphocytes (mouse or human) did not exhibit SWAC transients. SWAC influx could be distinguished from the calcium release-activated Ca^{2+} (CRAC) influx pathway stimulated by store depletion with TG. In TG-treated thymocytes, $[Ca^{2+}]_i$ rose steadily for ≈100 s, peaked at ≈900 nM, and then declined slowly. Simultaneous activation of both pathways produced an additive $[Ca^{2+}]_i$ profile. Gd^{3+} and La^{3+} blocked Ca^{2+} entry during CRAC activation more potently (K_d's of 28 and 58 nM, respectively) than Ca^{2+} influx during SWAC transients. SWAC transients could be elicited in the presence of 1 μM Gd^{3+}, after the complete inhibition of CRAC influx. Finally, whereas SWAC transients were principally restricted to immature thymocytes, TG stimulated the CRAC influx pathway in all four thymic CD4/CD8 subsets and in mature T cells. We conclude that SWAC and CRAC represent separate pathways for Ca^{2+} entry in thymocytes.

INTRODUCTION

Activation of the T-cell receptor/CD3 complex of lymphocytes by antigen, mitogenic lectins, or monoclonal antibodies initiates a rise in the concentration of intracellular free Ca^{2+} ($[Ca^{2+}]_i$). The rise in $[Ca^{2+}]_i$ is subdivided into two periods:

Address corresponcence to Dr. Michael D. Cahalan, Department of Physiology and Biophysics, University of California at Irvine, Irvine, California 92717.

J. GEN. PHYSIOL. © The Rockefeller University Press · 0022-1295/95/09/415/30 $2.00
Volume 106 September 1995 415–444

the first is brief and correlates with the release of stored Ca^{2+} triggered by inositol-1,4,5-triphosphate ($InsP_3$) (Berridge, 1993). The second results from sustained Ca^{2+} influx across the plasma membrane. Putney (1990) has speculated that Ca^{2+} influx is modulated indirectly by the Ca^{2+} content of $InsP_3$-sensitive stores by a process termed capacitative Ca^{2+} entry. This hypothesis suggests that the release of Ca^{2+} from pools activates a mechanism which initiates Ca^{2+} influx across the plasma membrane. In lymphocytes, the sustained influx of Ca^{2+} through "calcium release-activated" channels is a prerequisite for IL-2 gene expression (Negulescu, Shastri, and Cahalan, 1994) and T-cell proliferation (Crabtree and Clipstone, 1994).

Lewis and Cahalan (1989) first identified the Ca^{2+} influx pathway in T cells. In whole-cell, patch-clamp experiments, cytosolic dialysis of Jurkat T lymphocytes with pipette solutions containing EGTA or BAPTA activated a Ca^{2+}-selective current; the same current was recorded in cells stimulated with phytohemagglutinin (PHA) during perforated-patch experiments (Lewis and Cahalan, 1989). Strong buffering also stimulated Ca^{2+} influx in rat thymocytes (Montero, Alvarez, and Garcia-Sancho, 1990; Mason, Mahaut-Smith, and Grinstein, 1991*b*), at which time it was proposed that the degree of store filling dictated Ca^{2+} permeability in lymphocytes. Subsequent work, using specific inhibitors of ER Ca^{2+}ATPases to disrupt the balance between store refilling and depletion, revealed a Ca^{2+} influx pathway in many lymphoid cell types (Gouy, Cefai, Christensen, Debré, and Bismuth, 1990; Mason, Garcia-Rodriguez, and Grinstein, 1991*a*; Mason et al., 1991*b*; Sarkadi, Tordai, Homolya, Scharff, and Gardos, 1991). These Ca^{2+} influx pathways in T cells closely resemble calcium release-activated Ca^{2+} (CRAC) channels in rat mast cells (Hoth and Penner, 1992, 1993). Ca^{2+} influx through CRAC channels, or close relatives, is believed to underlie T-cell activation (Zweifach and Lewis, 1993; Premack, McDonald, and Gardner, 1994).

Other pathways for Ca^{2+} influx in T lymphocytes have been partially characterized. Two studies provide evidence for voltage-gated Ca^{2+} channels during whole-cell recordings in specific T-lymphocyte cell lines (Dupuis, Héroux, and Payet, 1989; Densmore, Szabo, and Gray, 1992). However, voltage-gated Ca^{2+} channels are not commonly expressed in lymphocytes; membrane depolarization with high K^+ extracellular solutions fails to elicit Ca^{2+} influx in Jurkat and human peripheral blood (HPB) T lymphocytes (references listed in Lewis and Cahalan, 1995). Another potential Ca^{2+} influx pathway, mediated by the direct interaction of $InsP_3$ with plasma membrane $InsP_3$-receptor channels, has been observed in cloned human T lymphocytes and Jurkat cells (Kuno, Goronzy, Weyand, and Gardner, 1986; Kuno and Gardner, 1987). A separate study using immunocytochemistry confirmed the presence of $InsP_3$ receptors on the surface of intact Jurkat T cells (Khan, Steiner, Klein, Schneider, and Snyder, 1992). Nevertheless, the functional role of plasma membrane, $InsP_3$-gated channels in lymphocytes is unclear at this time (Premack et al., 1994).

Many vertebrate cells exhibit a rise in $[Ca^{2+}]_i$ when challenged with other stimuli, such as hypoosmotic solutions (McCarty and O'Neil, 1992; Hoffmann, Simonsen, and Lambert, 1993). Depending upon cell type, this increase in $[Ca^{2+}]_i$ during swelling may result from $[Ca^{2+}]_i$ release, Ca^{2+} influx, or a combination of both

mechanisms. Stretch-activated cation channels are presumed to be the route for Ca^{2+} entry across the plasma membrane (Morris, 1990). After the rise in $[Ca^{2+}]_i$, separate K^+ and Cl^- efflux pathways are activated; in many cases, the K^+ and Cl^- conductances are directly modulated by $[Ca^{2+}]_i$. Within minutes, the loss of KCl and osmotically obliged water shrinks cells back to control volume by a process termed regulatory volume decrease (RVD). However, this sequence of events does not occur in HPB T lymphocytes, which display no change in $[Ca^{2+}]_i$ during swelling (Rink, Sanchez, Grinstein, and Roth, 1983; Grinstein and Smith, 1990). Rather, a Ca^{2+}-independent RVD mechanism has been proposed (Cahalan and Lewis, 1988; Deutsch and Lee, 1988; Rotin, Mason, and Grinstein, 1991), which begins with the opening of plasma membrane Cl^- channels in response to swelling. Membrane depolarization caused by the efflux of Cl^- from the cell activates voltage-gated K^+ channels. As before, the loss of KCl and water returns the lymphocyte to normal volume. At present, the Ca^{2+}-independent RVD hypothesis has been accepted as the mechanism used by lymphoid cells to resist conditions that cause swelling.

In this study, we report a novel Ca^{2+} influx pathway, activated by swelling, in certain populations of murine thymocytes. The swelling response in single cells is characterized by a sharp, transient rise in $[Ca^{2+}]_i$. These swelling-activated $[Ca^{2+}]_i$ (SWAC) transients are due to Ca^{2+} influx across the plasma membrane. Phenotypic analysis with CD4 and CD8 antibodies illustrates that SWAC influx is primarily associated with immature thymocytes. We compared SWAC influx in thymocytes to CRAC influx, which was stimulated by emptying Ca^{2+} stores with the microsomal Ca^{2+}-ATPase inhibitor thapsigargin (TG). Based upon kinetics, pharmacology, and phenotyping, we conclude that SWAC and CRAC represent distinct Ca^{2+} entry pathways through the plasma membrane of thymocytes. Furthermore, we suggest that Ca^{2+}-dependent channel activation may contribute to RVD in immature thymocytes.

Preliminary reports of this work have been published in abstract form (Ross, 1991; Ross and Cahalan, 1995).

MATERIALS AND METHODS

Lymphocyte Preparation and Fura-2 Loading

Thymectomies were performed on 4- to 10-wk old female Balb/c mice. Thymus glands were gently dissociated between two sintered glass microscope slides. Thymocytes were washed free of supporting tissue with RPMI 1640 media (GIBCO/BRL, Gaithersburg, MD) containing 10% fetal calf serum (JR Scientific, Woodland, CA), 25 mM HEPES and 2 mM glutamine (RPMI/10% FCS). The suspension was then centrifuged at 350 *g* for 10 min. An analogous protocol was used to isolate splenocytes from murine spleens. Cells were resuspended in RPMI/10% FCS, and aliquots containing $\approx 6 \times 10^6$ cells/ml were loaded with 3 μM fura-2/AM (Molecular Probes, Inc., Eugene, OR) for 20 min. After loading, lymphocytes were washed three times with RPMI/10% FCS and stored in the dark for up to 10 h before experiments. Cell preparation, dye loading, storage, and experiments were performed at room temperature (≈22°C).

HPB T lymphocytes were purified from the blood of healthy adult donors as described previously (Hess, Oortgiesen, and Cahalan, 1993). Experiments were also performed on Jurkat E6-1 cells, a human T leukemic cell line, obtained from the American Type Culture Collection (Rock-

ville, MD) and maintained in RPMI/10% FCS media following standard procedures. HPB and Jurkat T lymphocytes were loaded with fura-2/AM as described above.

Solutions

Mammalian Ringer solution contained (in millimolar): 160 NaCl, 4.5 KCl, 2 $CaCl_2$, 1 $MgCl_2$, and 5 HEPES, titrated to pH 7.4 with NaOH. Hypoosmotic solutions were prepared by diluting 100% Ringer with distilled water. 10 mM glucose was added to isoosmotic and diluted Ringer solutions before experiments.

Cytosolic Calcium Measurements and Fura-2 Calibration

Lymphocytes were allowed to settle onto glass coverslip chambers pretreated with 0.5 mg/ml poly-D-lysine (Sigma Chemical Co., St. Louis, MO) for 10 min. Adhered cells were then washed with Ringer on the stage of a Zeiss Axiovert 35 microscope (Carl Zeiss, Oberkochen, Germany). A xenon arc lamp (Carl Zeiss) provided the light for imaging fura-2 in lymphocytes at 360- and 380-nm wavelengths; the light passed through a motorized filter wheel/shutter assembly (Lambda 10, Axon Instruments, Inc., Foster City, CA) containing 360- and 380-nm excitation filters (Omega Optical, Brattleboro, VT) and was reflected by a 400-nm dichroic mirror through a 100× oil-immersion objective (Zeiss Neofluar) to illuminate dye-loaded cells. Dye fluorescence was monitored above 480 nm with a Hamamatsu C2400 SIT camera (Hamamatsu Photonics, Bridgewater, NJ) connected to a video image-processing system (Videoprobe, ETM Systems, Irvine, CA). At 5-s intervals, 8-bit images, averaged over 16 frames, were collected at 360- and 380-nm wavelengths. The background-subtracted pixel intensities of the 360- and 380-nm images were divided in register to give 360/380 ratios, which were stored digitally. $[Ca^{2+}]_i$ in intact cells was calculated from 360/380 ratios using the equation of Grynkiewicz, Poenie, and Tsien (1985):

$$[Ca^{2+}]_i = K_d(F_{min}/F_{max})(R - R_{min})/(R_{max} - R) \quad (1)$$

where K_d is the dissociation constant for fura-2 in the cytosol (250 nM), F_{min} and R_{min} are the 380-nm fluorescent intensity and 360/380 ratio at low $[Ca^{2+}]_i$, F_{max} and R_{max} are the 380-nm fluorescence intensity and 360/380 ratio at high $[Ca^{2+}]_i$, and R is the 360/380 ratio recorded during experiments. Calibration measurements of F_{min} and R_{min} were performed after incubating cells for 10 min in nominally Ca^{2+}-free Ringer containing 2 mM EGTA. Cells were then superfused with Ringer containing 1 μM TG, 5 μM ionomycin, and 10 mM Ca^{2+} to evaluate F_{max} and R_{max}.

During osmotic swelling, the concentration of dye within cells is reduced, and the surrounding cytoplasmic viscosity may also decline. Botchkin and Matthews (1993) have described a potential artifact of fura-2 measurements in swollen retinal pigment epithelial cells, leading to a small apparent increase in $[Ca^{2+}]_i$ (≈100 nM). This apparent rise, calculated from the ratio of 340 and 380 nm fura-2 fluorescence, was due mostly to a decrease in 380 nm fluorescence. In HPB T cells, the observed apparent rise of 50 nM upon exposure to hypoosmotic solution may originate from this artifact. The SWAC transients described in this paper may be influenced by, but do not originate from, this artifact for three reasons as described in Results. First, the SWAC transients are much larger in amplitude and do not parallel the time course of volume changes. Second, they can be eliminated by acute removal of Ca^{2+} and by the addition of lanthanides or organic blockers. Third, during SWAC transients, the 350 nm fluorescence rises as the 380 nm fluorescence falls (not shown).

Single-Cell Volume Determination

We employed a custom-designed beam-splitter to separate the green fluorescence emission of fura-2 loaded cells from a differential interference contrast (DIC) image illuminated with red light, similar in concept to the method of Foskett (1988). Cross over between DIC and fluores-

cence images was insignificant and therefore allowed the near-simultaneous measurement of volume and $[Ca^{2+}]_i$ within single cells. After beam-splitter partition, the light signals were collected by two separate cameras. The process of data storage limited the acquisition of each pair of DIC and fluorescence images to intervals of 7 s. $[Ca^{2+}]_i$ in single cells was calculated as described above, while single-cell outlines in digitized DIC images were traced manually using NIH Image v1.57ppc, a Macintosh computer program written by Wayne Rasband at the National Institutes of Health and available from the Internet by anonymous ftp from zippy.nimh.nih.gov or on floppy disc from NTIS, 5285 Port Royal Rd., Springfield, VA 22161, part no. PB93-504868. Relative volume (V/V_0) was calculated from cross-sectional surface areas before (S_0) and during swelling (S) with the relation

$$V/V_0 = (S/S_0)^{3/2} \quad (2)$$

This relationship assumes a spherical cell.

Single-Cell Phenotyping and $[Ca^{2+}]_i$ Measurements

In some experiments, murine thymocytes were labeled with CD4 (L3T4) and CD8 (Lyt-2) monoclonal antibodies (Becton Dickinson Corp., San Jose, CA), conjugated with the fluorescent compounds phycoerythrin (PE) or fluorescein isothiocyanate (FITC), respectively. Cells were incubated on ice with 2.5 μg/ml anti-CD4-PE and anti-CD8-FITC for 20 min. After staining, cells were washed three times with cold RPMI/10% FCS, resuspended to a final volume of 400 μl, and then stored on ice until needed. Subsequent experiments were performed with 50-μl aliquots of stained cells that had been allowed to adhere to poly-D-lysine-coated coverslips for 15 min.

Light from a xenon arc-lamp (see above), passing through sets of filters optimized for fluorescent color separation and directed through a 100× oil-immersion objective, illuminated the antibody-labeled cells. A 510- to 560-nm excitation filter, a 580-nm dichroic beam splitter, and a 590-nm long-pass emission filter comprised the anti-CD4-PE filter set. The anti-CD8-FITC filter set contained a 450- to 490-nm excitation filter, a 510-nm dichroic beam splitter, and a 40-nm-wide emission filter centered at 540 nm. Discrimination between red and green fluorescence images was verified using PE- and FITC-labeled Calibrite beads (Becton-Dickinson Corp.).

Subset classification of thymocytes was performed with epifluorescence photomicroscopy. Separate photographs of red and green fluorescent thymocytes were recorded on Ektachrome P1600 film (Eastman Kodak Corp., Rochester, NY). A third brightfield image, using condenser illumination, was also photographed. Cells were then loaded with 3 μM fura-2/AM for 20 min on the microscope stage. $[Ca^{2+}]_i$ measurements were performed on the phenotyped cells as described above. Photographic images classified thymocytes into four categories: (*a*) fluorescently labeled cells exhibiting both red and green fluorescence (double positive, $CD4^+CD8^+$); (*b*) cells exhibiting red fluorescence (single positive, $CD4^+CD8^-$); (*c*) cells exhibiting green fluorescence (single positive, $CD4^-CD8^+$); and (*d*) colorless, unlabeled thymocytes (double negative, $CD4^-CD8^-$), that appeared only in brightfield images. Thymocyte phenotype was correlated with single-cell $[Ca^{2+}]_i$ measurements after the photographs were developed.

Materials

Stock solutions of fura-2/AM and TG (LC Services, Woburn, MA) were dissolved in dimethyl sulfoxide (DMSO) as 1 mM concentrations and stored at −20°C. The metal salts $NiCl_2 \cdot 6H_2O$, $GdCl_3 \cdot 6H_2O$, $LaCl_3 \cdot 6H_2O$ (Alfa/Johnson Matthey Co., Ward Hill, MA), and $CdCl_2 \cdot 2.5H_2O$ (Mallinckrodt, St. Louis, MO) were dissolved in Ringer as 100 mM stocks. Nicardipine, nifedipine, and methoxyverapamil (D-600) were purchased from Sigma Chemical Co. and dissolved in ethanol as 10 mM stocks. All other chemicals were from Sigma Chemical Co.

Data Analysis

Exponential curves were fitted to the decay of $[Ca^{2+}]_i$ transients with an Apple Macintosh computer program (Igor Pro v2.02, WaveMetrics, Inc., Lake Oswego, OR). Statistical analysis was performed with Excel v5.0 (Microsoft, Redmond, WA), SuperAnova v1.11 (Abacus Concepts, Inc., Berkeley, CA), and Systat v5.1 (Systat Inc., Evanston, IL). Grouped data are reported as mean ± SD, unless otherwise indicated. Mean values were compared by analysis of variance; pairs of means were considered statistically different if P was <0.05.

RESULTS

Results are divided into four sections. First, we describe $[Ca^{2+}]_i$ transients in swollen murine thymocytes. Second, we examine the influx pathway activated by depleting intracellular Ca^{2+} stores. Third, we provide evidence that separate pathways are activated during swelling and store depletion. And finally, we show that SWAC transients are principally associated with immature lymphocyte subsets.

SWAC Transients in Thymocytes

Fluorescence-ratio imaging of fura-2-loaded murine thymocytes during swelling revealed rapid changes in $[Ca^{2+}]_i$ at the single-cell level (Fig. 1 *A*). Superfusion of thymocytes with hypoosmotic solution (60% of isoosmotic) elicited a rise in $[Ca^{2+}]_i$ from the resting level of 101 ± 8 nM ($n = 6$ experiments, 652 cells) to a peak of 646 ± 213 nM. On average, 77 ± 4% ($n = 6$ experiments, 857 cells) of thymocytes exhibited $[Ca^{2+}]_i$ transients during swelling. $[Ca^{2+}]_i$ rose steeply from resting to peak levels within 10 s in the majority of cells eliciting SWAC transients. A histogram showing the distribution of latencies between the hypoosmotic solution change and peak $[Ca^{2+}]_i$ for 652 cells is displayed in Fig. 1 *B*. The average latency is 70 ± 29 s. No significant correlation is present between the amplitude of $[Ca^{2+}]_i$ transients and latency (Fig. 1 *C*).

The decay of each SWAC transient was fitted by a single exponential function. The average time constant for decay was 20 ± 10 s ($n = 6$ experiments, 652 cells). The decline in $[Ca^{2+}]_i$ from peak to basal levels is primarily due to cytosolic Ca^{2+} buffering and Ca^{2+} pumps in the plasma membrane and endoplasmic reticulum (Scharff and Foder, 1993). However, 8 min after the hypoosmotic solution exchange, $[Ca^{2+}]_i$ remained elevated at 167 ± 23 nM, a level that is significantly higher than resting $[Ca^{2+}]_i$ ($P < 0.01$). This elevated $[Ca^{2+}]_i$ may indicate that Ca^{2+} influx continues through SWAC or other pathways at a rate sufficient to overload buffering and pump-down mechanisms.

Lymphocytes require ≈60 s to reach maximum volume when swollen with hypoosmotic solution (Cheung, Grinstein, Dosch, and Gelfand, 1982*a*; Grinstein, Cohen, Sarkadi, and Rothstein, 1983; Grinstein, Rothstein, Sarkadi, and Gelfand, 1984). We also examined the relationship between $[Ca^{2+}]_i$ and volume in thymocytes during swelling (Fig. 2 *A*). SWAC transients were observed as single cells attained their maximal volume. Peak values in average $[Ca^{2+}]_i$ and V/V_o profiles show alignment at ≈60 s (Fig. 2 *C*). A minority of thymocytes display no change in $[Ca^{2+}]_i$ during swelling. At the start of experiments, nonresponsive thymocytes were indistinguishable from cells exhibiting transients; resting $[Ca^{2+}]_i$ in nonre-

sponsive cells averaged 105 ± 13 nM (n = 6 experiments, 205 cells). However, nonresponsive cells (Fig. 2 *B*) swelled to a greater volume and exhibited a longer delay before the inception of RVD, as compared to thymocytes exhibiting SWAC transients (cf. average V/V_o traces in Fig. 2 *C*). Furthermore, nonresponsive thymocytes were more swollen after 9 min in hypoosmotic media and shrank less when isoos-

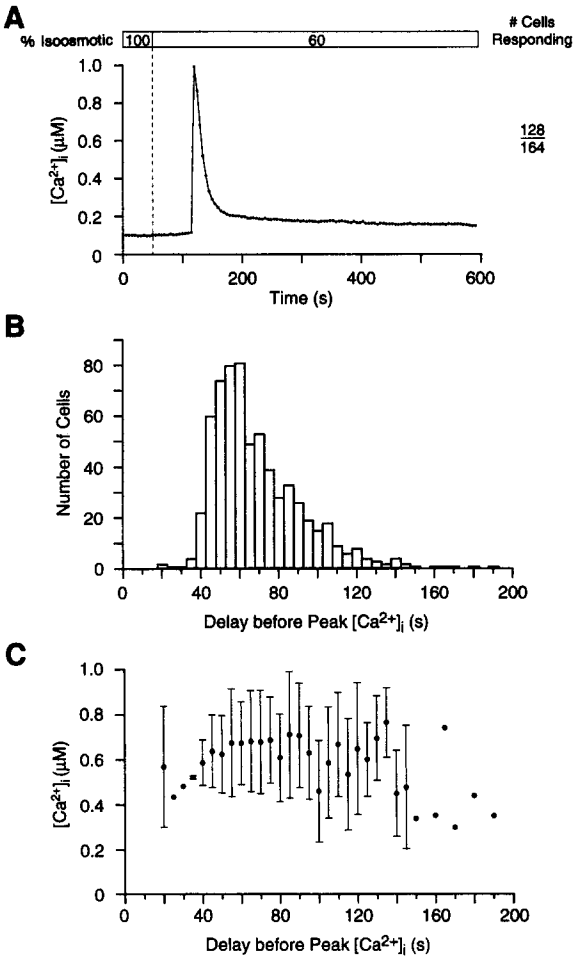

FIGURE 1. Mouse thymocytes exhibit $[Ca^{2+}]_i$ transients during swelling. Individual cells were classified into two subgroups; thymocytes exhibiting transients and those showing little change in $[Ca^{2+}]_i$ over 10 min. (*A*) $[Ca^{2+}]_i$ is plotted against time for a single cell showing a SWAC transient. The time course includes experimental data (*separate points*) taken at 5-s intervals. The horizontal bar above the graph indicates the osmolarity of the extracellular solution (relative to isoosmotic mammalian Ringer), whereas the vertical dashed line shows the time of solution exchange. Typically, 20 s was necessary to complete the solution exchange. Reported delays include this 20-s lag period. Conventions used here apply to subsequent figures (experiment 43094-4; cell 53). (*B*) A latency histogram for thymocytes exhibiting SWAC transients is plotted for 652 cells (77% of total population). Latency (s) was calculated as the time interval between the start of hypoosmotic solution application and peak $[Ca^{2+}]_i$ during SWAC transients. Histogram bins are 5-s wide and correlate with the frequency of data collection (experiments 43094-1 to 43094-6; 652 cells). (*C*) Peak $[Ca^{2+}]_i$ plotted against the latency period shows no correlation. Symbols represent mean peak $[Ca^{2+}]_i$ for binned data, while error bars indicate ± SD.

motic media was reapplied (Fig. 2 *C*). Table I summarizes these differences. These results suggest that SWAC transients in thymocytes enhance RVD.

Ca^{2+} influx is required for SWAC transients. SWAC transients were never observed in the absence of extracellular Ca^{2+}, suggesting that Ca^{2+} influx underlies $[Ca^{2+}]_i$ transients (Fig. 3 *A*). By exposing cells briefly to Ca^{2+}-free solutions, we ex-

amined and ruled out the possibility that rapid depletion of intracellular Ca^{2+} stores in Ca^{2+}-free media could suppress the SWAC response (Fig. 3 *B*). SWAC transients were recorded in only 6 ± 2% ($n = 2$ experiments, 159 cells) of the cells, and these responses were initiated before Ca^{2+} withdrawal. The subsequent addition of ionomycin released intracellular Ca^{2+}, demonstrating that stores contained Ca^{2+} well after the peak SWAC response in the latency histogram (see Fig. 1 *B*). In Fig. 3 *C*, the length of Ca^{2+} exposure during swelling was extended to 60 s, resulting in a greater percentage of thymocytes (49%) eliciting SWAC transients. These results

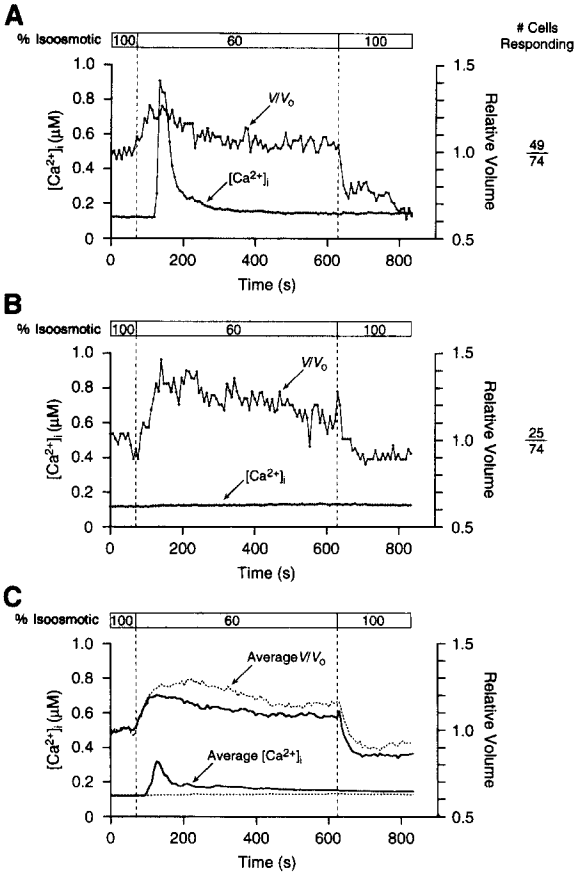

FIGURE 2. Peak $[Ca^{2+}]_i$ during the SWAC transient and maximum swollen volume are temporally correlated. (*A*) $[Ca^{2+}]_i$ and relative volume (V/V_o) are plotted against time for a single cell showing a SWAC transient. The time courses include experimental data (*separate points*) taken at 7-s intervals (experiment 12595-3; cell 9. (*B*) A minority of thymocytes show very little change in $[Ca^{2+}]_i$ during the experiment. However, RVD is exhibited in the V/V_o time course (experiment 12595-5; cell 4). (*C*) Average $[Ca^{2+}]_i$ and V/V_o are plotted against time for cells showing transients (*solid lines*) and nonresponsive thymocytes (*dashed lines*). The asynchronous initiation of SWAC transients in single cells broadens the average time course (experiments 12595-3 to 12595-6).

indicate that SWAC transients depend critically on Ca^{2+} influx.

We performed experiments to determine, in relation to cell swelling, the period during which SWAC transients can be elicited in thymocytes. As shown in Fig. 4 *A*, cells were exposed to Ca^{2+}-free, isoosmotic media for 5 min before swelling. After this incubation period, thymocytes were swollen in Ca^{2+}-free media for 60 s. Readdition of Ca^{2+} elicited SWAC transients in 64% of the thymocytes. The percentage of thymocytes displaying SWAC transients decreased as the period of swelling in Ca^{2+}-free media lengthened (Fig. 4 *B*). These findings illustrate that the SWAC re-

TABLE I

Change in Thymocyte Volume during Swelling

	Thymocytes exhibiting SWAC transients (49 cells)	Thymocytes not showing SWAC transients (25 cells)
Maximum V/V_o	1.31 ± 0.10	1.44 ± 0.11
V/V_o at 600 s	1.08 ± 0.10	1.15 ± 0.14
V/V_o after isoosmotic shrinkage	0.86 ± 0.09	0.92 ± 0.07

Changes in relative volume (V/V_o) during swelling were measured in single cells. Representative traces are shown in Fig. 2. Data are presented as mean ± SD. Pairs of means were significantly different at $P < 0.01$. Data collected from four experiments (experiments 12595-3 to 12595-6).

sponse is restricted to a short window of time (≈3 min). Summary histograms for Fig. 3, *B* and *C*, and Fig. 4, *A* and *B*, are shown in Fig. 4, *C* and *D*, respectively. The temporal profile of these histograms, in combination with data presented in Figs. 1 *B*, and 2, *A* and *C*, suggest that the window of opportunity coincides with maximal

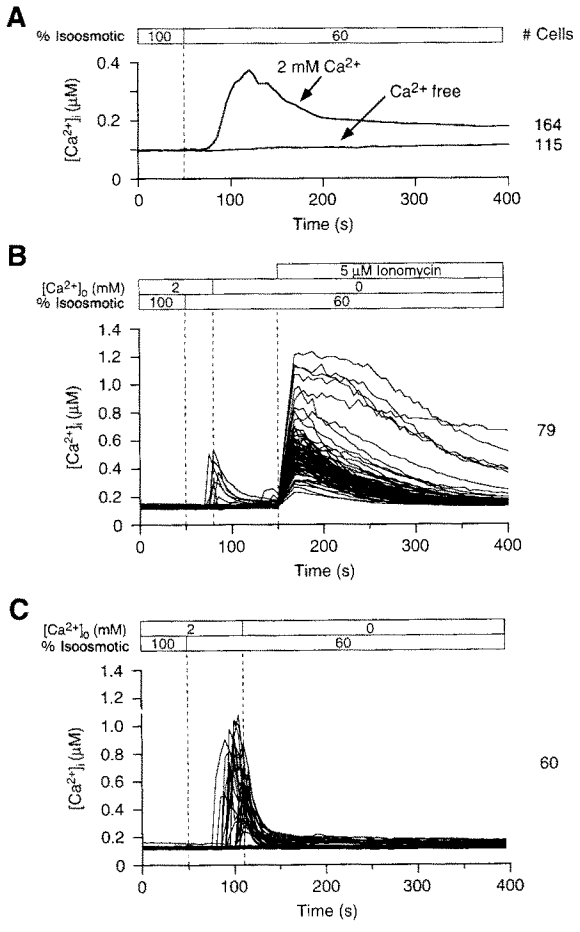

FIGURE 3. Ca^{2+} influx is required for SWAC transients. (*A*) Average $[Ca^{2+}]_i$ profiles for thymocytes swollen in the presense and absence of 2 mM Ca^{2+}. SWAC transients were recorded in 78% of the cells swollen in the presence of Ca^{2+}, while no $[Ca^{2+}]_i$ change was observed when thymocytes were swollen in Ca^{2+}-free media (experiments 43094-4 and 41394-8). (*B*) Intracellular Ca^{2+} stores are not involved in the generation of SWAC transients. Single cell $[Ca^{2+}]_i$ profiles are displayed. During the first 30 s of swelling, thymocytes were exposed to 2 mM Ca^{2+}. After this brief exposure, the bathing media was replaced with hypoosmotic, Ca^{2+}-free Ringer. Few cells elicited SWAC transients. 5 μM ionomycin added at 150 s in Ca^{2+}-free, hypoosmotic media revealed that intracellular stores contained Ca^{2+} (experiment 12595-16). (*C*) Longer exposure to 2 mM Ca^{2+} during swelling increases the percentage of thymocytes displaying SWAC transients. Single-cell $[Ca^{2+}]_i$ profiles are shown (experiment 12595-10).

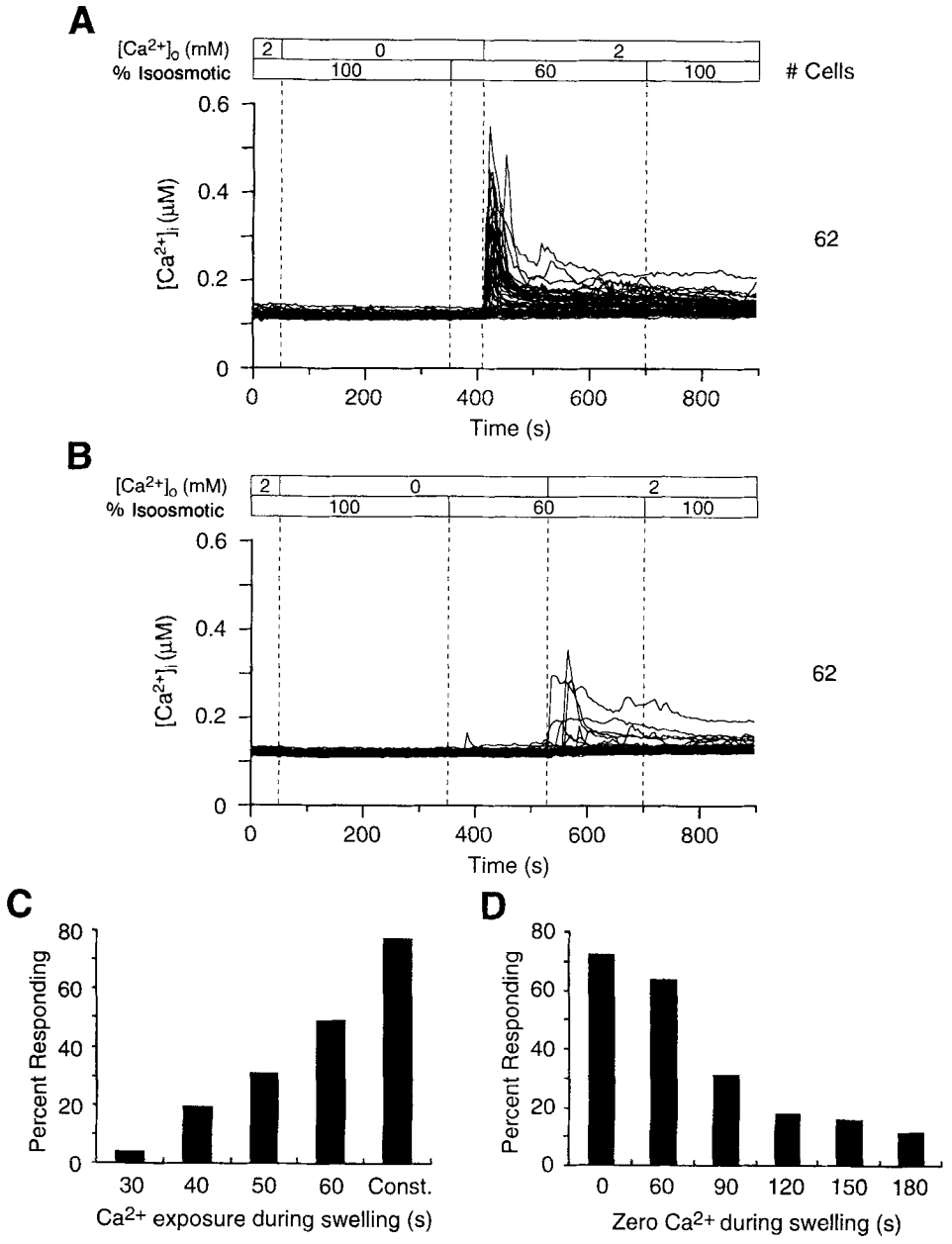

FIGURE 4. Thymocytes require Ca^{2+} during a critical period to elicit SWAC transients. (*A*) 64% of thymocytes preswollen for 60 s in Ca^{2+}-free media exhibit SWAC transients. $[Ca^{2+}]_i$ profiles are displayed for 62 individual cells (experiment 12495-6). (*B*) When held in Ca^{2+}-free hypoosmotic media for longer periods, fewer cells exhibit SWAC transients (experiment 12495-2). (*C*) Summary histogram of data presented in Fig. 3, *B* and *C*. As the period of Ca^{2+} exposure during swelling is lengthened, a greater percentage of thymocytes show SWAC transients. *Const.* (*far right bar*) indicates

cellular volume. Furthermore, Fig. 4 reinforces the conclusion that SWAC transients are the result of Ca^{2+} influx, rather than the release of stored Ca^{2+}.

Pharmacology. We next examined the ability of Ca^{2+}-channel antagonists to inhibit SWAC influx. Ca^{2+} influx pathways in a wide range of cell types are blocked by polyvalent metal cations and organic compounds (Tsien and Tsien, 1990; Hille, 1992). Trivalent cations of the lanthanide series inhibited SWAC influx effectively.

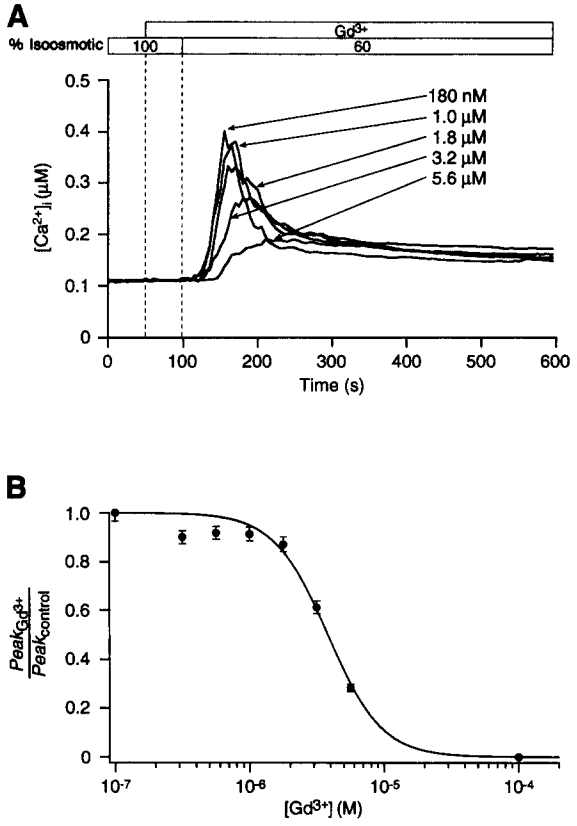

FIGURE 5. SWAC transients are blocked by µM Gd^{3+}. (*A*) Average $[Ca^{2+}]_i$ profile of five experiments at increasing Gd^{3+} concentrations (experiments 43094-46, 43094-51, 43094-54, 43094-56, and 43094-57) (*B*) Gd^{3+} dose-response curve for SWAC transients. The degree of Gd^{3+} block in single cells was calculated by dividing peak $[Ca^{2+}]_i$ in the presence of Gd^{3+} ($Peak_{Gd3+}$) by average peak $[Ca^{2+}]_i$ measured during control experiments ($Peak_{control}$). Two experiments were performed at each Gd^{3+} concentration. Data points represent the mean fraction of peak $[Ca^{2+}]_i$, with error bars indicating ± SEM. The data was fitted with a Hill equation of the form, $Peak_{Gd3+}/Peak_{control} = 1/[1 + ([Gd^{3+}]_0/K_d)^{n_h}]$, where K_d is the half-blocking concentration of Gd^{3+} (3.8 µM), and n_h is the Hill coefficient (2) (experiments 43094-43 to 43094-58).

Fig. 5 *A* displays the average time course of five experiments conducted with increasing concentrations of extracellular Gd^{3+} ($[Gd^{3+}]_o$). The traces show a concentration-dependent decrease in the average amplitude of SWAC transients from 787 ± 287 nM (180 nM Gd^{3+}, $n = 2$ experiments, 176 cells) to 287 ± 131 nM (5.6 µM Gd^{3+}, $n = 2$ experiments, 180 cells). In Fig. 5 *A*, note that the time courses exhibited significantly higher $[Ca^{2+}]_i$ after Gd^{3+} application than at rest. A high

that Ca^{2+} was present during the entire hypoosmotic exposure (experiments 12595-7 to 12595-10, and 43094-1 to 43094-6). (*D*) Summary histogram of data presented in *A* and *B*. The percentage of cells exhibiting SWAC transients decreases as the period of exposure to Ca^{2+}-free, hypoosmotic media increases (experiments 12495-2 to 12495-6, and 12495-8).

$[Gd^{3+}]_o$ of 100 μM was necessary to lower $[Ca^{2+}]_i$ back to basal levels. This finding supports the idea that another Ca^{2+} influx pathway, which is less sensitive to $[Gd^{3+}]_o$, develops concurrently with SWAC influx during swelling. A Gd^{3+} dose-response curve for SWAC influx is shown in Fig. 5 *B*. Separate data points were best fit using a K_d of 3.8 μM and a Hill coefficient (n_h) of 2. La^{3+} was slightly more effective at blocking SWAC influx; the dose-response curve for La^{3+} yielded a K_d of 2.4 μM (data not shown). Potent lanthanide inhibition of the SWAC response reinforces the conclusion that Ca^{2+} influx mediates $[Ca^{2+}]_i$ transients.

Divalent transition metal cations and dihydropyridine Ca-channel antagonists were less effective blockers. Ni^{2+} inhibited SWAC influx with a K_d of 4.4 mM (data not shown). Cd^{2+} was effective at levels >100 μM. Similarly, 100 μM levels of nifedipine, D-600, and nicardipine inhibited SWAC influx.

Swollen thymocytes respond in a threshold-like manner. We measured the degree of swelling needed to trigger $[Ca^{2+}]_i$ transients by superfusing thymocytes with stepwise-diluted Ringer solutions. The osmolarity of the bathing media was decreased in 10% increments at 3-min intervals. $[Ca^{2+}]_i$ transients were recorded in 84 ± 4% of thymocytes (n = 3 experiments, 451 cells) using this stepwise dilution protocol. $[Ca^{2+}]_i$ profiles in three individual cells (Fig. 6, *A–C*) illustrate the range of re-

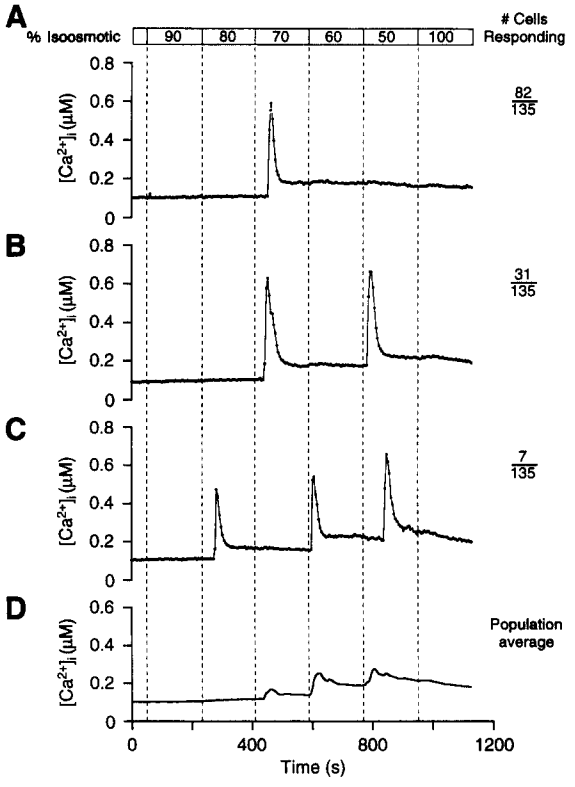

FIGURE 6. Stepwise dilution of extracellular solution can elicit multiple SWAC transients in single cells. Ringer was diluted by steps of 10% at 3-min intervals. (*A*) $[Ca^{2+}]_i$ plotted against time for a thymocyte displaying a single transient after the step to 70% isoosmotic. Most thymocytes exhibited single transients, but not until the solution change to 60% isoosmotic was complete (experiment 43094-7; cell 97). (*B*) A single cell displaying a pair of SWAC transients. This cell exhibited transients after steps to 70 and 50% isoosmotic. Typically, one dilution step separated SWAC transients in thymocytes exhibiting doublets (experiment 43094-7; cell 103). (*C*) $[Ca^{2+}]_i$ time course showing three transients during the dilution run. The first transient in this cell, elicited after the step to 80% isoosmotic, set the upper limit of osmotic sensitivity in thymocytes (experiment 43094-7; cell 42). (*D*) The composite average of 135 thymocytes shows a rise in steady state $[Ca^{2+}]_i$ with each dilution step below 70% isoosmotic (experiment 43094-7).

sponses. While a few thymocytes exhibited a single SWAC transient of normal amplitude and duration after the step to 70% isoosmotic (Fig. 6 *A*), the majority of cells responded at 60% isoosmotic. Solutions more dilute than 50% caused many thymocytes to burst, as previously reported (Cheung et al., 1982*a*; Cheung, Grinstein, and Gelfand, 1982*b*).

Approximately 30% of cells exhibited more than one transient during the dilution run (Fig. 6, *B* and *C*). Most cells exhibiting doublets responded at 70% isoosmotic with the first transient of the pair, while the second was elicited after the step to 50% isoosmotic (Fig. 6 *B*). This finding suggests that a recovery period, longer than the 3-min interval between dilution steps, is typically required before secondary transients can be generated. A few thymocytes displayed three or four transients during the experiment (Fig. 6 *C*). The step to 80% isoosmotic proved to be the upper limit of sensitivity. Theoretically, in 80% Ringer, thymocytes would swell in vol-

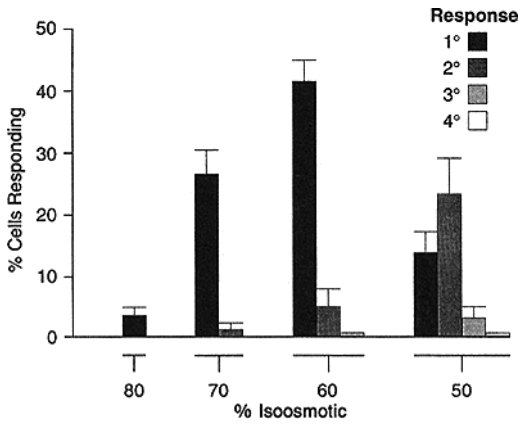

FIGURE 7. Histogram summarizing $[Ca^{2+}]_i$ transients in thymocytes during stepwise dilution experiments. Transients are classified by the level of hypoosmolarity (*horizontal axis*) and their relative position to one another in single-cell $[Ca^{2+}]_i$ profiles (*legend*). Primary responses (*black bars*) indicate the dilution step at which the first transient in a single cell was generated. Note that successive responses (secondary, tertiary and quaternary) in each hypoosmolarity category do not always correlate with the preceding dilution step (e.g., a cell showing a secondary response at 60% isoosmotic may have given a primary response at either 80 or 70%). Error bars, some of which are too small to be seen, indicate ± SD (experiments 110393-2, 43094-7, and 43094-8).

ume by 125% if they behaved as perfect osmometers. Thymocytes consistently showed a ≈70 nM rise in steady state $[Ca^{2+}]_i$ after transients decayed (Fig. 6, *A–C*). Multiple transients in single cells led to progressively higher steady state $[Ca^{2+}]_i$ (Fig. 6, *B* and *C*). The average time course (Fig. 6 *D*) demonstrates that steady state $[Ca^{2+}]_i$ rises with each reduction in osmolarity beyond 70%.

Fig. 7 presents a histogram of $[Ca^{2+}]_i$ transients grouped according to the dilution of the extracellular solution. The step to 70% isoosmotic triggers $[Ca^{2+}]_i$ transients reliably in swollen thymocytes; predictable secondary transients do not occur until thymocytes are challenged with bathing media diluted by 50%. We never observed more than one transient in thymocytes challenged with a single hypoosmotic step (e.g., see Figs. 1 *A* and 2 *A*). However, repeated exposure to the same hypoosmotic solution, with an isoosmotic recovery period separating each exposure, elicited multiple transients in a few thymocytes (<5%, data not shown).

CRAC Influx in Thymocytes

The main objectives of this study were to characterize SWAC transients in thymocytes and distinguish SWAC influx from other Ca^{2+} entry pathways. To address this second issue, we examined the influx of Ca^{2+} through the CRAC pathway in TG-treated thymocytes. TG specifically inhibits microsomal Ca^{2+}-ATPases, exposing an endogenous leak pathway which empties stores (for review, see Thastrup, Dawson, Scharff, Foden, Cullen, Drøbak, Bjerrum, Christensen, and Hanley, 1989), leading to Ca^{2+} influx by capacitative Ca^{2+} entry (Putney, 1990).

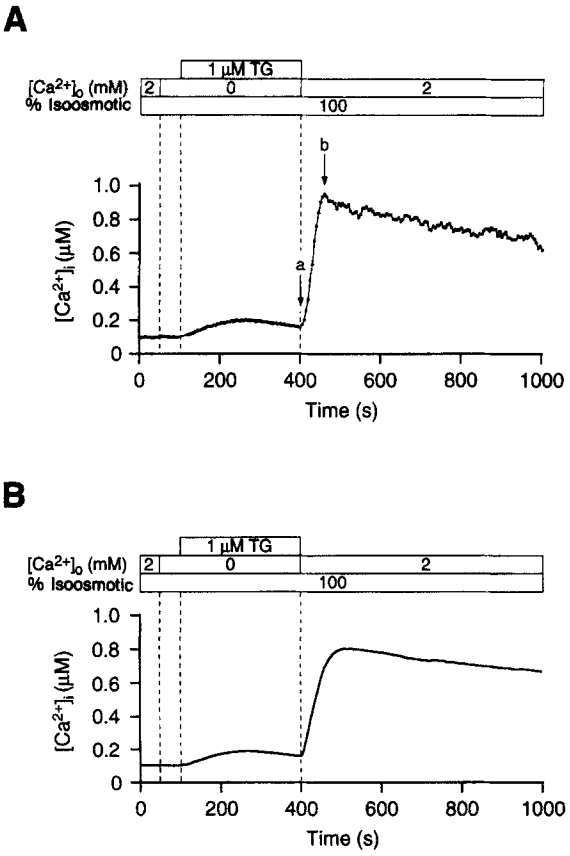

FIGURE 8. Depletion of intracellular Ca^{2+} stores stimulates CRAC influx in TG-treated thymocytes. (*A*) Single-cell response showing release of stored Ca^{2+} between 100 and 400 s. Reapplication of extracellular Ca^{2+} at 400 s activates CRAC influx. A slowly declining plateau develops after $[Ca^{2+}]_i$ has reached maximal levels. Labeled arrows indicate start and end points over which time derivatives were calculated (experiment 42794-5; cell 75). (*B*) The average time course is displayed for 107 cells (experiment 42794-5).

Fig. 8 illustrates a protocol making it possible to separate Ca^{2+} release and Ca^{2+} influx within single cells. After a 50-s incubation period in Ca^{2+}-free media, a saturating dose of TG (1 μM; Gouy et al., 1990) was applied to thymocytes. $[Ca^{2+}]_i$ rose immediately after TG treatment, and on average required 167 ± 42 s (n = 25 experiments, 2,925 cells) to reach a maximum value of 208 ± 31 nM. Maximum $d[Ca^{2+}]/dt$ during release averaged 1.1 ± 0.6 nM/s. After TG-sensitive stores were exhausted, buffering and TG-insensitive Ca^{2+} pumps gradually lowered $[Ca^{2+}]_i$. Ca^{2+} readdition to Ca^{2+}-depleted thymocytes caused $[Ca^{2+}]_i$ to increase rapidly,

peaking after 103 ± 71 s (n = 1 experiment, 107 cells) at a value of 905 ± 144 nM. Maximum $d[Ca^{2+}]/dt$, typically measured at the midpoint of the rise, averaged 21 ± 15 nM/s. This value is equivalent in magnitude to the initial rate of increasing $[Ca^{2+}]_i$ in the presence of 2 mM Ca^{2+} (≈17 nM/s) measured by Premack et al. (1994) in TG-treated Jurkat T cells. The rising phase in thymocytes halted abruptly, leading to a steady state which declined gradually at −0.35 ± 0.16 nM/s.

Extracellular Ca^{2+} dependence. The decline in $[Ca^{2+}]_i$ after the peak represents the interplay between Ca^{2+} influx through the CRAC pathway, cytosolic Ca^{2+} buffering, Ca^{2+} extrusion via plasma membrane Ca^{2+} pumps, and Ca^{2+} sequestration by TG-insensitive Ca^{2+} pumps. We examined the declining phase by exposing thymocytes to multiple Ca^{2+}-free episodes. Fig. 9, *A* and *C*, illustrates that $[Ca^{2+}]_i$ falls after each exposure to Ca^{2+}-free media. However, each time Ca^{2+} is reapplied, $[Ca^{2+}]_i$ rises near to the previous peak level. The slope of the tangent line drawn in Fig. 9 *A* was less steep than the decline measured in Fig. 8. We also measured the

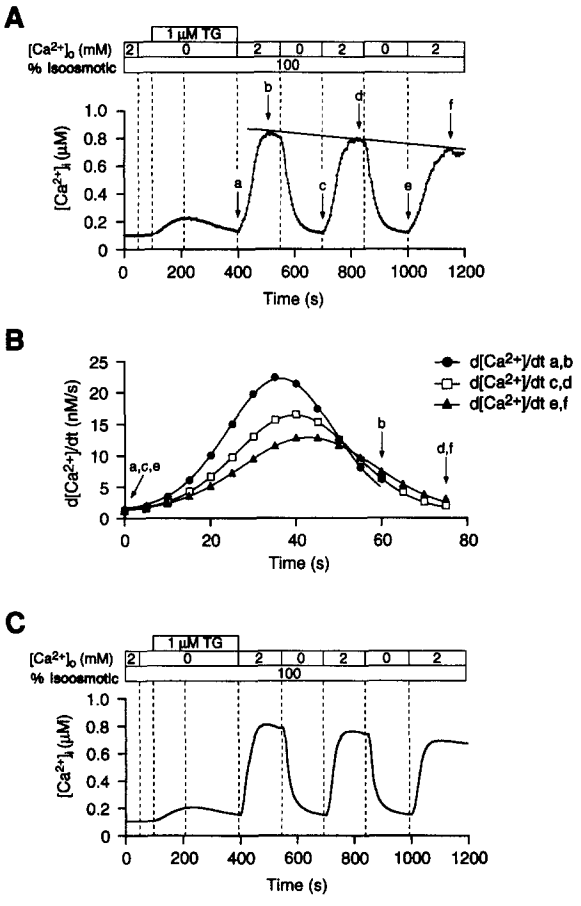

FIGURE 9. CRAC influx depends upon extracellular Ca^{2+}. (*A*) $[Ca^{2+}]_i$ time course in a single cell exposed to Ca^{2+}-free cycles spaced at regular intervals of 300 s. Ca^{2+}-free Ringer solution rapidly lowers $[Ca^{2+}]_i$; however, $[Ca^{2+}]_i$ almost reaches previous peak levels after Ca^{2+} is reapplied. The tangent line drawn between $[Ca^{2+}]_i$ peaks at arrows *b*, *d*, and *f* exhibits a slope of −0.26 nM/s (experiment 51394-8; cell 16). (*B*) $d[Ca^{2+}]/dt$ during Ca^{2+} exposure declines with successive Ca^{2+}-free episodes. Labeled arrows correspond to those in *A*. Between arrows *a* and *b*, maximum $d[Ca^{2+}]/dt$ in this cell reached 22.4 nM/s. Maximum $d[Ca^{2+}]/dt$ then fell to 16.5 nM/s during the second cycle. Finally, between arrows *e* and *f*, maximum $d[Ca^{2+}]/dt$ decreased to 12.8 nM/s. (*C*) Average response of 109 cells. Peak $[Ca^{2+}]_i$ fell from 847 ± 170 nM (n = 2 experiments, 239 cells) to 808 ± 154 nM, finally reaching 744 ± 145 nM during the last cycle. Peak levels were established 93 ± 42 s after the first Ca^{2+} readdition, then at 83 ± 39 s and 87 ± 39 s during subsequent cycles. These numbers were used to calculate an average declining slope of −0.17 nM/s between peaks (experiment 51394-8).

rise in $d[Ca^{2+}]/dt$ during the three influx episodes; time derivatives are shown in Fig. 9 *B*. On average, maximum $d[Ca^{2+}]/dt$ decreased from 23 ± 15 nM/s to 18 ± 10 nM/s, indicating that declining peak $[Ca^{2+}]_i$ during the influx episodes correlates with slower $d[Ca^{2+}]/dt$.

Lanthanide block. Like SWAC transients, the influx of Ca^{2+} through the CRAC pathway is sensitive to lanthanides (see above and Mason et al., 1991*b*; Demaurex,

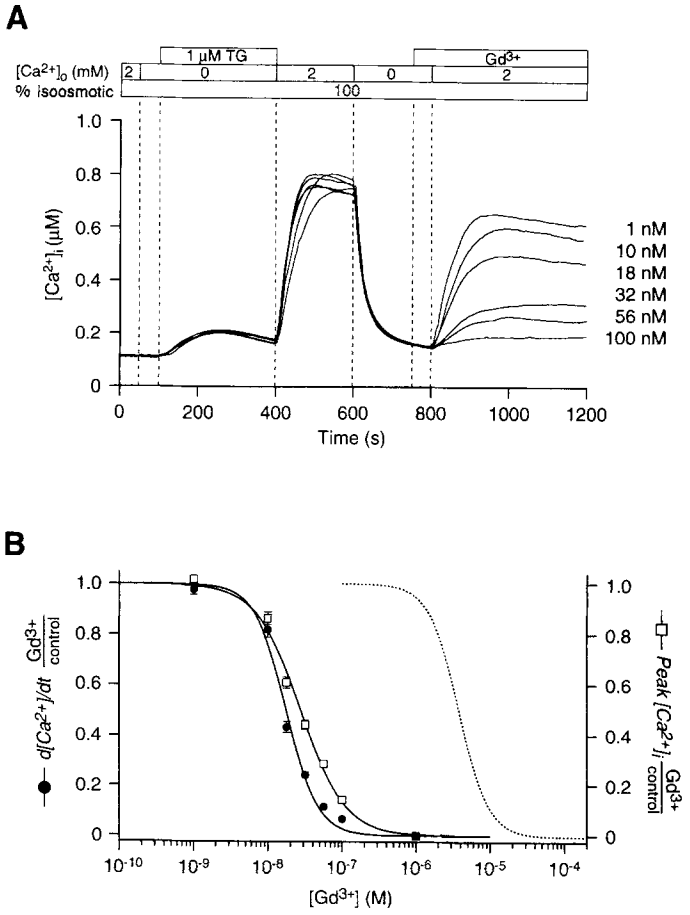

FIGURE 10. CRAC influx in thymocytes is blocked by nM Gd^{3+}. (*A*) Average $[Ca^{2+}]_i$ profile of six experiments at increasing Gd^{3+} concentrations. The CRAC influx episode between 400 and 600 s was used as an internal control. Average responses are the composite of >100 cells (experiments 51594-5, 51594-10, 51594-11, 51594-13, 51594-16, and 51594-17). (*B*) Gd^{3+} dose-response curves for CRAC influx (*solid lines*). The degree of block was calculated as the ratio of $d[Ca^{2+}]/dt$ before and after Gd^{3+} application with the following equation: $d[Ca^{2+}]/dt$, (Gd^{3+}/control) = $[(Slope_{800\text{–}1000s}/Slope_{400\text{–}600s})/(Slope_{episode\ 2}/Slope_{episode\ 1})]$, where $Slope_{400\text{–}600s}$ is maximum $d[Ca^{2+}]/dt$ during the internal control (see *A*), and $Slope_{800\text{–}1000s}$ is maximum $d[Ca^{2+}]/dt$ between 800 and 1000 s. Successive $d[Ca^{2+}]/dt$ measurements during control experiments are signified by $Slope_{episode\ 1}$ and $Slope_{episode\ 2}$, respectively. The amount of block was calculated from peak $[Ca^{2+}]_i$ measurements with an analogous equation. Data points represent mean values, with error bars indicating ± SEM. In some

TABLE II

Lanthanide Block Summary

		K_d		n_h	
		La^{3+}	Gd^{3+}	La^{3+}	Gd^{3+}
SWAC transients	Peak	2.4 μM	3.8 μM	2.0	2.0
CRAC influx	Slope	33 nM	18 nM	1.5	2.0
	Peak	58 nM	28 nM	1.5	1.5

See Figs. 5 and 10 legends for an explanation of K_d and n_h measurements.

Lew, and Krause, 1992; Hoth and Penner, 1993). In Fig. 10, we provide evidence that nanomolar amounts of Gd^{3+} or La^{3+} block Ca^{2+} entry through the CRAC pathway in thymocytes. Experiments measuring the block of CRAC influx are complicated by mechanisms which regulate $[Ca^{2+}]_i$. As described above, the declining $[Ca^{2+}]_i$ plateau is controlled by at least four parameters: Ca^{2+} influx, buffering, sequestration, and extrusion. Therefore, to examine a preferential blocking effect on influx, inhibitors must be added before $[Ca^{2+}]_i$ rises. Because $d[Ca^{2+}]/dt$ in thymocytes varies during CRAC activation, an internal control must be established for each cell before applying blocker. In Fig. 10 *A*, the internal control in the absence of inhibitor corresponds to the interval between 400 and 600 s. Two independent assessments of block are provided by this experiment: a change in $d[Ca^{2+}]/dt$, and effects on peak $[Ca^{2+}]_i$. Gd^{3+} has a similar effect on $d[Ca^{2+}]/dt$ and peak $[Ca^{2+}]_i$; thus, we can infer that Gd^{3+} primarily blocks Ca^{2+} influx through the CRAC pathway in thymocytes. In Fig. 10 *B*, we have plotted two Gd^{3+} dose-response curves (*solid lines*; Fig. 5 *B*, *dotted line*). A Hill equation fitted the ratio of $d[Ca^{2+}]/dt$ measurements before and after Gd^{3+} application with a K_d of 18 nM and n_h of 2. Similarly, a Hill equation fitted to fractional peak $[Ca^{2+}]_i$ exhibited a K_d of 28 nM and n_h of 1.5. Therefore, Gd^{3+} blocks Ca^{2+} entry through the CRAC pathway ≈130 times more effectively than it inhibits Ca^{2+} influx during SWAC transients (cf. Fig. 5, Results). La^{3+} was slightly less effective than Gd^{3+} at blocking CRAC influx (data not shown). A summary of K_d and n_h values for Gd^{3+} and La^{3+} block of SWAC and CRAC pathways is presented in Table II. Whereas Gd^{3+} blocks CRAC influx more effectively than La^{3+}, the opposite is true for the inhibition of SWAC transients.

Separate Ca^{2+} Influx Pathways

SWAC transients can be generated after stores are emptied. Our pharmacology data suggest that SWAC and CRAC are separate pathways. The following experiments (Figs. 11–13) provide further evidence that the pathways are distinct. Most thymocytes (59%) swollen immediately after TG treatment elicit $[Ca^{2+}]_i$ transients (Fig. 11 *A*). After a delay of 57 ± 42 s (n = 1 experiment, 70 cells), $[Ca^{2+}]_i$ during

cases, data symbols cover error bars. A Hill equation of the form $d[Ca^{2+}]/dt$, (Gd^{3+}/control) = $1/[1 + ([Gd^{3+}]_o/K_d)^{n_h}]$ fitted the slope data (*filled circles*) with a K_d of 18 nM and n_h of 2. Peak data (*open squares*) were fitted with a K_d of 28 nM and n_h of 1.5. The Gd^{3+} dose response curve for block of SWAC transients from Fig. 5 *B* (*dotted line*) is plotted as a reference (experiments 51594-5 to 51594-18).

SWAC transients peaked at a higher level (1,208 ± 159 nM) than reported earlier without store depletion (see Fig. 1). Thymocytes exhibiting SWAC transients displayed a much slower rise in CRAC influx than nonresponsive thymocytes (cf. Figs. 11 *A* and 11 *B*). Elevated $[Ca^{2+}]_i$ is believed to stimulate Ca^{2+}-ATPases and/or inhibit depletion-activated Ca^{2+} influx in lymphocytes (Lewis and Cahalan, 1989; Dolmetsch and Lewis, 1994; Premack et al., 1994) and in A431 cells, a human cancer

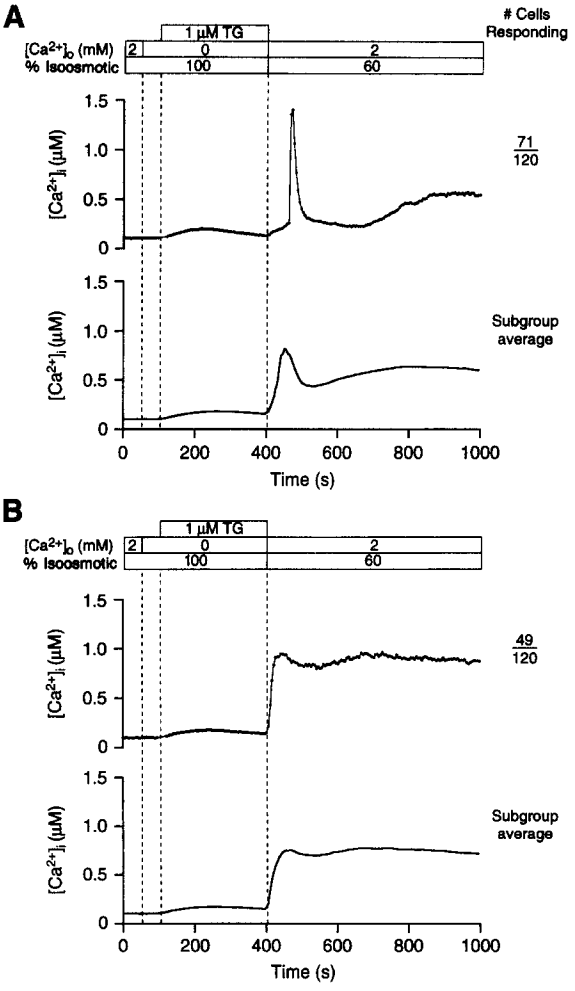

FIGURE 11. SWAC transients are not affected by depletion of TG-sensitive, intracellular stores. (*A*) A subgroup of 71 cells (59% of total) exhibited $[Ca^{2+}]_i$ transients immediately after store depletion. Note the extended delay in the single-cell $[Ca^{2+}]_i$ profile (*top*) and subgroup average (*bottom*) before $[Ca^{2+}]_i$ transients. After the transient peak, $[Ca^{2+}]_i$ decayed with a time constant averaging 22 ± 16 s and reached a minimum of 402 ± 135 nM (experiment 42794-6; cell 16). (B) Subgroup of thymocytes not displaying $[Ca^{2+}]_i$ transients (experiment 42794-6; cell 35).

cell line derived from epidermal tissue (Lückhoff and Clapham, 1994). The transient elevation of $[Ca^{2+}]_i$ generated by SWAC influx may stimulate one or both of these processes and delay the development of CRAC influx in thymocytes.

Ca^{2+} influx pathways are additive. Shown in Fig. 12 *A* is the simultaneous generation of CRAC and SWAC influxes in a single cell. Less than half (46 ± 4%, $n = 2$ experiments, 223 cells) of the thymocytes elicited SWAC transients above the $[Ca^{2+}]_i$ plateau established by CRAC influx. The low percentage of thymocytes ex-

hibiting transients suggests that the SWAC response is inhibited by elevated $[Ca^{2+}]_i$ during the plateau. After a delay of 60 ± 16 s, $[Ca^{2+}]_i$ reached 1,184 ± 178 nM (n = 2 experiments, 99 cells) during the transients, and then decayed with a time constant of 19 ± 7 s. As in Fig. 11 *A*, depletion of TG-sensitive stores correlated with substantially higher peak $[Ca^{2+}]_i$ during transients. Likewise, $[Ca^{2+}]_i$ rose slowly after the superimposed transient (Fig. 12 *A*).

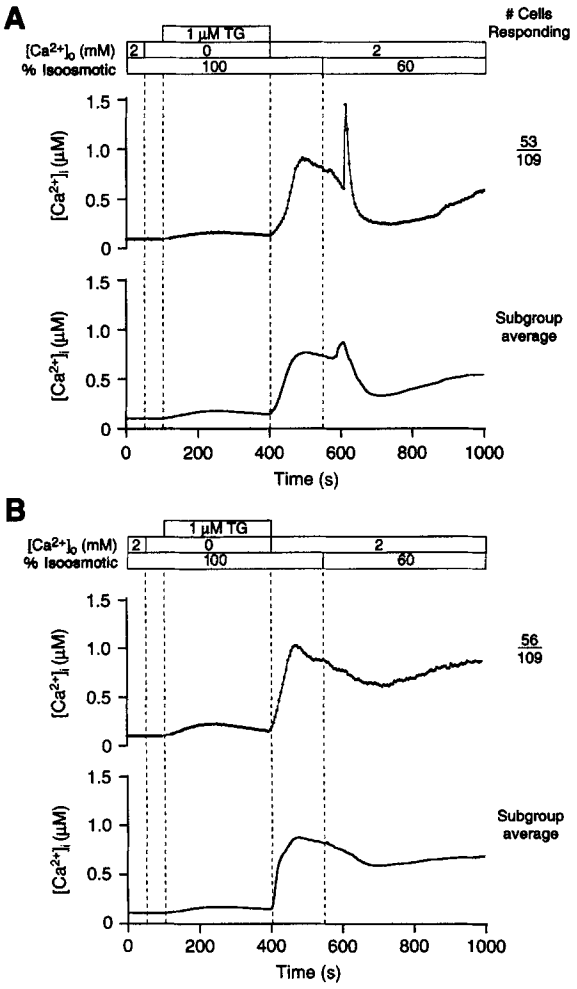

FIGURE 12. SWAC and CRAC influxes are additive. (*A*) Thymocyte subgroup (49% of total) displaying SWAC transients after the development of CRAC influx. The single-cell time course (*top*) and average response (*bottom*) suggest that the rise in $[Ca^{2+}]_i$ caused by SWAC influx inhibits CRAC activation (experiment 42794-4, cell 36). (*B*) Subgroup of thymocytes not exhibiting $[Ca^{2+}]_i$ transients (experiment 42794-4, cell 35).

Pharmacological separation. Three lines of evidence support the hypothesis that SWAC and CRAC influx pathways are distinct: (*a*) $d[Ca^{2+}]/dt$ kinetics differ substantially between the two pathways; (*b*) the pathways differ in sensitivity to lanthanide block; and (*c*) the pathways are additive and can be activated simultaneously in single cells. In Fig. 13, the two Ca^{2+} influx pathways are distinguished by their relative Gd^{3+} sensitivity. After the depletion of Ca^{2+} stores with TG, $[Ca^{2+}]_i$

was allowed to rise for 100 s (between 400 and 500 s in Fig. 13, *A* and *B*). Maximum $d[Ca^{2+}]/dt$ reached 15 ± 7 nM/s ($n = 1$ experiment, 88 cells) before $[Ca^{2+}]_i$ peaked at 750 ± 206 nM after a 92 ± 12 s delay. The delay measurement indicates that $[Ca^{2+}]_i$ in most cells plateaued before Gd^{3+} application at 500 s. CRAC influx was completely blocked by 1 μM Gd^{3+}; $[Ca^{2+}]_i$ declined with a time constant of 37 ± 13 s, a value significantly longer than that measured during the sequential

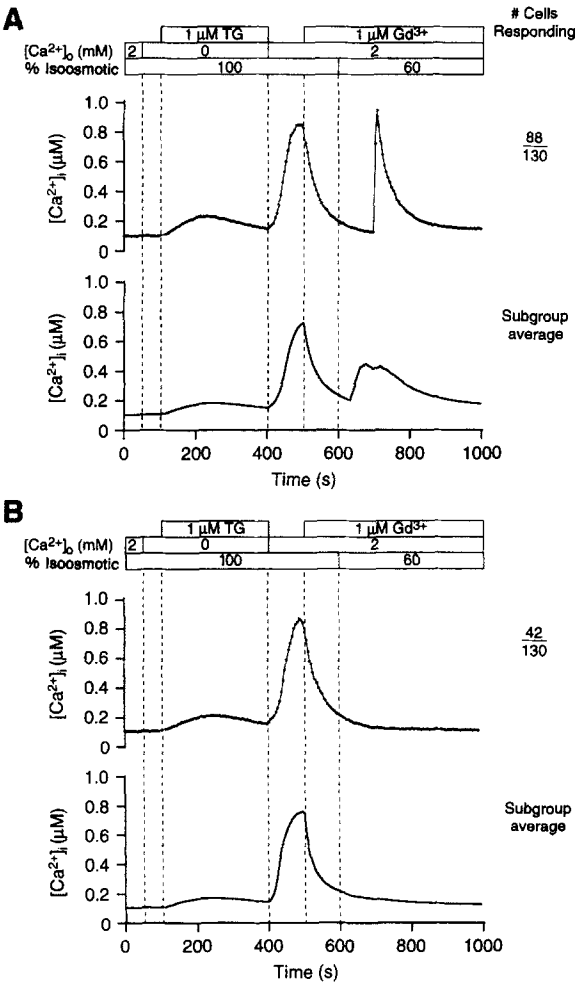

FIGURE 13. SWAC transients can be generated after Gd^{3+} block of Ca^{2+} influx through the CRAC pathway. (*A*) 68% of the thymocytes swollen in the presence of 1 μM Gd^{3+} displayed SWAC transients after the complete inhibition of CRAC influx (experiment 42794-13; cell 52). (*B*) Subgroup of 42 cells exhibiting CRAC influx, but not SWAC transients (experiment 42794-13; cell 2).

Ca^{2+}-free episodes in Fig. 9. Therefore, Ca^{2+} pumps in the plasma membrane of thymocytes are sensitive to $[Gd^{3+}]_o$ in the μM range. Lanthanide inhibition of plasma membrane Ca^{2+} pumps has been reported previously in various cell types (Kwan, Takemura, Obie, Thastrup, and Putney, 1990; Carafoli, 1991).

Hypoosmotic solution applied at 600 s generated SWAC transients in 68% of the cells. A delay of 75 ± 29 s was measured before $[Ca^{2+}]_i$ transients; $[Ca^{2+}]_i$ peaked at

663 ± 168 nM and then declined with a time constant averaging 63 ± 48 s. This experiment demonstrates that SWAC transients can be observed in the presence of 1 μM Gd^{3+}, after the complete inhibition of CRAC influx. A similar experiment can be performed with 0.5 μM La^{3+} (data not shown), even though a narrower K_d margin for La^{3+} block (41-fold) separated SWAC and CRAC influxes.

T-Cell Phenotyping

SWAC transients correlate with thymocyte phenotype. Using fluorescently labeled monoclonal antibodies, we examined the surface expression of CD4 and CD8 on thymocytes before swelling. Developmental stages in thymocytes were then correlated with their ability to elicit SWAC transients. Table III summarizes the phenotyping experiments. The results indicate that immature double-negative and double-positive thymocytes are more likely to exhibit SWAC transients than single-positive $CD4^+CD8^-$ (helper) and $CD4^-CD8^+$ (cytotoxic/suppressor) cells. Representative single-cell $[Ca^{2+}]_i$ traces of the four CD4/CD8 phenotypes are displayed in Fig. 14 *A*. The presence of surface antibodies did not affect the ability of thymocytes to elicit a response; 69 ± 10% (n = 14 experiments, 815 cells) of pheno-

TABLE III

CD4/CD8 Surface Expression Correlated with SWAC Transients in Murine Thymocytes

CD4/CD8	Percent of total	Percent exhibiting transients
−/−	7	78 ± 23
+/+	68	84 ± 9
+/−	20	33 ± 17
−/+	5	13 ± 17

Mean values were compared with a one-way ANOVA and the statistical difference between pairs of means evaluated with a Tukey-Kamer post-hoc test. Pairs of means were significantly different at $P < 0.05$, except −/− vs +/+. Data collected from 14 experiments: −/− phenotype, 56 cells; +/+ phenotype, 555 cells; +/− phenotype, 161 cells; −/+ phenotype, 43 cells (experiments 70594-2 to 70594-5; 70994-1 to 70994-8, 70994-13, and 70994-14).

typed cells exhibited SWAC transients. SWAC transients were most frequently observed in double-positive thymocytes. The $CD4^-CD8^+$ subgroup was least likely to exhibit transients. In contrast, the four phenotypes displayed identical $[Ca^{2+}]_i$ profiles during CRAC influx (Fig. 14 *B*). Our data represent a "snapshot" of thymocytes at various developmental stages. Many thymocytes were probably observed in transition between phenotypes. Further distinction among the four thymocyte subpopulations, based upon the relative fluorescence brightness of bound CD4 and CD8 antibodies or the expression of other surface markers, was not performed. Nevertheless, these results support the hypothesis that SWAC transients are primarily associated with immature thymocyte phenotypes.

Mature T cells fail to exhibit SWAC transients. To address the proposal that $[Ca^{2+}]_i$ transients are more often seen in immature lymphocyte populations, we examined $[Ca^{2+}]_i$ responses in swollen murine splenocytes and HPB T cells. Peripheral lymphocytes share many properties with mature thymocytes. Therefore, single-positive CD4/CD8 thymocytes, or closely related subgroups, are thought to be precursors

of peripheral T cells. Fig. 15 *A* shows a typical splenocyte $[Ca^{2+}]_i$ profile (*top*) and the average time course (*bottom*) during exposure to 60% isoosmotic solution. $[Ca^{2+}]_i$ profiles in most splenocytes displayed fluctuations rather than sharp, single transients. These $[Ca^{2+}]_i$ fluctuations, which varied in amplitude and frequency,

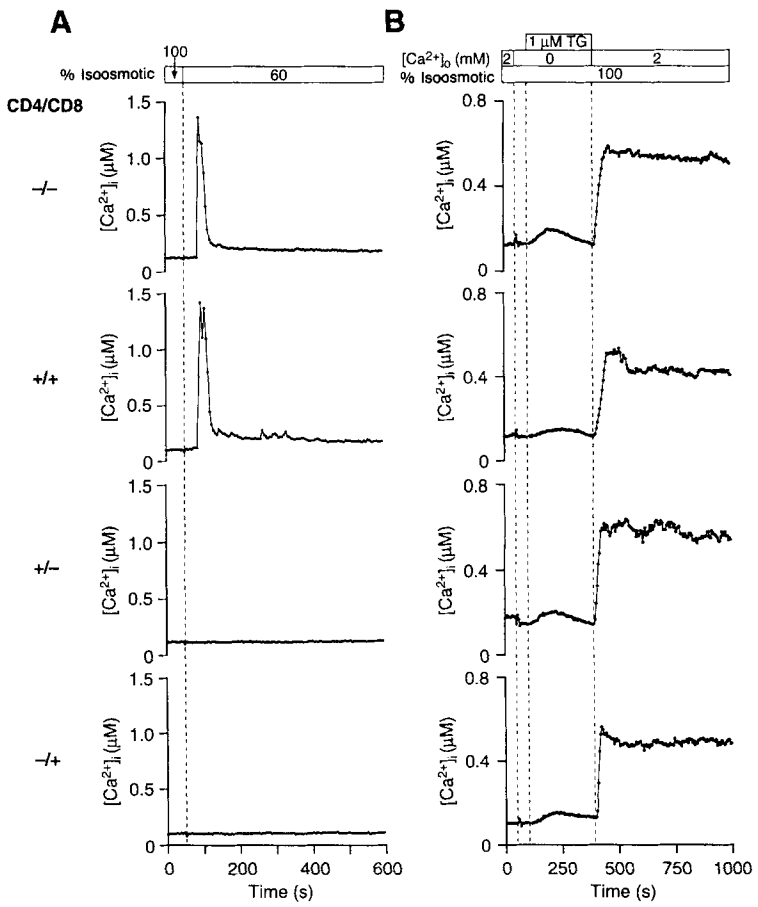

FIGURE 14. SWAC transients and thymocyte phenotype are correlated. (*A*) The majority of immature thymocytes exhibit SWAC transients during swelling. $[Ca^{2+}]_i$ time courses in four representative thymocytes, classified by surface expression of CD4 and CD8, show typical swelling-induced responses. Approximately 80% of immature thymocytes, designated −/− (double negatives) and +/+ (double positives), exhibit SWAC transients (see Table III). In contrast, most (>80%) of the mature thymocytes, classified as +/− and −/+ (single positives), show no response. (experiments 70994-8; cells 51, 54, 71, and 74). (*B*) TG stimulates Ca^{2+} influx through the CRAC pathway in all four classes of CD4/CD8 thymocytes. (experiment 70994-10; cells 6, 12, 19, and 68).

were stopped by returning cells to isoosmotic bathing media. A few splenocytes displayed $[Ca^{2+}]_i$ spikes immediately after the solution exchange to hypoosmotic media (e.g., Fig. 15 *A*, *top*). However, these spikes decayed completely to basal $[Ca^{2+}]_i$ levels, unlike SWAC transients in thymocytes which led to a sustained plateau above

resting $[Ca^{2+}]_i$ (see Figs. 1 *A*, and 2, *A* and *C*). HPB T cells (Fig. 15 *B*), like the subset of nonresponsive murine thymocytes described in Fig. 2 *B*, showed very little change in $[Ca^{2+}]_i$ during swelling.

We also examined the swelling-induced $[Ca^{2+}]_i$ response in Jurkat T lymphocytes, a cell line commonly used to study $[Ca^{2+}]_i$ signaling. Jurkat T cells (Fig. 15 *C*) display $[Ca^{2+}]_i$ fluctuations similar to those seen in swollen splenocytes (Fig. 15 *A*). However, large fluctuations in $[Ca^{2+}]_i$ were less frequent in Jurkat T cells, perhaps

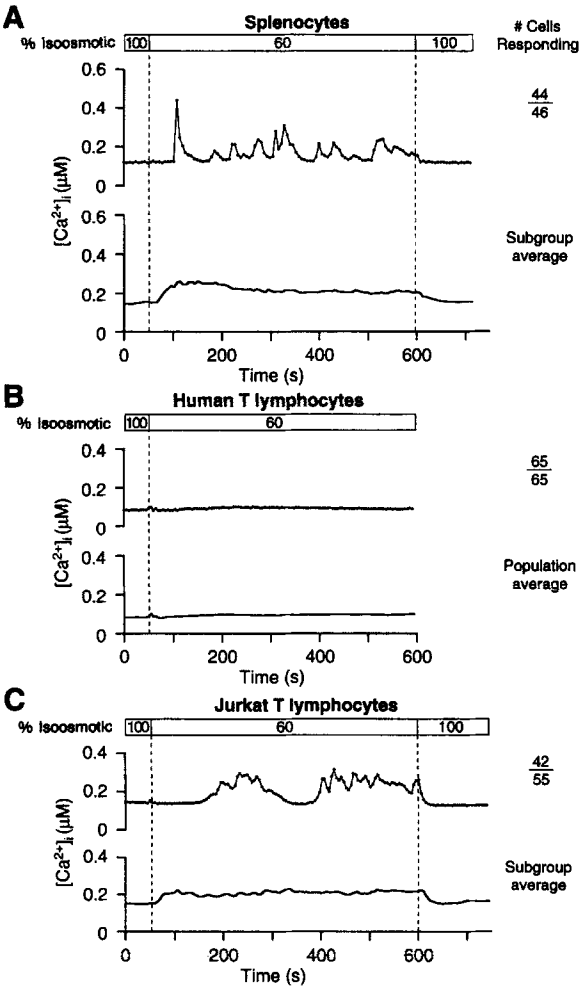

FIGURE 15. Mature lymphocytes do not exhibit SWAC transients. (*A*) Swollen splenocytes exhibit $[Ca^{2+}]_i$ fluctuations rather than sharp transients. Because $[Ca^{2+}]_i$ fluctuations in single cells (*top*) are asynchronous, the average profile (*bottom*) appears smooth. Reapplication of isoosmotic solution stops $[Ca^{2+}]_i$ fluctuations. On average, peak $[Ca^{2+}]_i$ in swollen splenocytes reached 388 ± 152 nM (n = 2 experiments, 91 cells) from a resting level of 141 ± 45 nM (n = 4 experiments, 234 cells). $[Ca^{2+}]_i$ decreased to 163 ± 43 nM (n = 2 experiments, 91 cells) with the return of isoosmotic media; this $[Ca^{2+}]_i$ level was not significantly different from basal measurements (experiment 120693-2; cell 35). (*B*) Human peripheral T cells show little change in $[Ca^{2+}]_i$ during swelling. From a resting level of 85 ± 13 nM (n = 3 experiments, 129 cells), average $[Ca^{2+}]_i$ in swollen HPB T lymphocytes reached 125 ± 48 nM before declining over a period of 8 min to 95 ± 25 nM. This small change in $[Ca^{2+}]_i$ during swelling may be artifactual. The apparent rise in $[Ca^{2+}]_i$ can be mimicked by a 10% decrease in the K_d of fura-2 from 250 to 225 nM as the cell swells (not shown) (experiment 41394-1; cell 53). (*C*) Swollen Jurkat T lymphocytes, like splenocytes, exhibit $[Ca^{2+}]_i$ fluctuations. However, fluctuations are less frequent and smaller in amplitude in Jurkat T lymphocytes. On average, $[Ca^{2+}]_i$ in swollen Jurkat T cells reached 387 ± 195 nM (n = 3 experiments, 200 cells) from a resting level of 144 ± 12 nM. Isoosmotic media attentuated $[Ca^{2+}]_i$ fluctuations and lowered $[Ca^{2+}]_i$ to 196 ± 70 nM (n = 2 experiments, 121 cells). Jurkat $[Ca^{2+}]_i$ images were recorded with a 63× objective (experiment 41394-5; cell 6).

due to their larger size. Furthermore, Jurkat T cells do not exhibit $[Ca^{2+}]_i$ spikes when first swollen. These $[Ca^{2+}]_i$ fluctuations may correlate with the inwardly directed "leak" conductance measured previously in whole-cell, patch-clamp recordings of swollen Jurkat T cells (Ross, Garber, and Cahalan, 1994).

DISCUSSION

In this study we have characterized a distinct Ca^{2+} influx pathway activated by cell swelling in immature mouse thymocytes. Features of the SWAC influx pathway include (*a*) a transient macroscopic $[Ca^{2+}]_i$ profile (Figs. 1, 2, 6, 11, 12, 13, and 14); (*b*) a critical dependence on extracellular Ca^{2+} (Figs. 3 and 4); and (*c*) block by μM amounts of Gd^{3+} and La^{3+} (Fig. 5 and Table II). The restriction of SWAC influx to immature T-cell subsets (Table III) is consistent with the absence of transients in swollen mouse splenocytes, HPB, and Jurkat T lymphocytes (Fig. 15 *A–C*). Comparison experiments indicate that thymocytes use separate pathways for SWAC and CRAC influx. Five lines of evidence support this finding: (*a*) $d[Ca^{2+}]/dt$ kinetics differ substantially between the two pathways (cf. Figs. 1 *A*, 2 *A*, and 8 *A*); (*b*) lanthanides blocked Ca^{2+} entry during CRAC activation much more potently than Ca^{2+} influx during SWAC transients (Figs. 5, 10, and Table II); (*c*) the simultaneous activation of both pathways generated an additive $[Ca^{2+}]_i$ profile in single cells (Fig. 12 *A*); (*d*) the difference in sensitivity to Gd^{3+} illustrated that SWAC transients could be elicited in the presence of 1 μM Gd^{3+}, after the complete inhibition of Ca^{2+} entry through the CRAC pathway (Fig. 13). Similar results were obtained with 0.5 μM La^{3+}, even though a narrower K_d margin for La^{3+} separated SWAC and CRAC inhibition (Table II); and finally (*e*) SWAC transients are primarily restricted to immature thymocytes, while TG stimulated the CRAC influx pathway in all four thymic CD4/CD8 subsets and in mature T cells (Figs. 14 and 15).

Ca^{2+} Dependence of RVD

Grinstein, Dupre, and Rothstein (1982) first hypothesized that a rise in $[Ca^{2+}]_i$ initiated RVD in swollen HPB T lymphocytes. They proposed that the opening of Ca^{2+}-activated K^+ (K_{Ca}) channels provides the cation efflux limb of RVD based on the following results: (*a*) A23187-treated cells shrank in isoosmotic media; (*b*) A23187 caused $K^+/^{86}Rb^+$ efflux to increase; (*c*) quinine (50–100 μM), believed at the time to block K_{Ca} channels specifically, inhibited RVD; (*d*) calmodulin inhibitors blocked A23187-induced cell shrinkage, $K^+/^{86}Rb^+$ efflux, and RVD; and (*e*) the RVD response in lymphocytes preincubated with Ca^{2+}-free/EGTA solutions was diminished. The authors speculated that, because of increased $^{45}Ca^{2+}$ efflux in swollen lymphocytes, Ca^{2+} release from stores stimulated RVD. Bui and Wiley (1981) had already determined that $^{45}Ca^{2+}$ uptake did not increase in swollen lymphocytes. The Ca^{2+}-release hypothesis was discounted when no change in $[Ca^{2+}]_i$ could be measured in swollen lymphocytes with the fluorescent Ca^{2+} indicator quin2 (Rink et al., 1983). Rink and coauthors (1983) noted that quin2 may have buffered Ca^{2+} and attenuated $[Ca^{2+}]_i$ changes in swollen lymphocytes. Nevertheless, RVD was observed in swollen, quin2-loaded lymphocytes.

As an alternative to K_{Ca} channels, voltage-gated K^+ (K_V) channels with overlap-

ping pharmacological sensitivity were proposed to underlie loss of K^+ during RVD (DeCoursey, Chandy, Gupta, and Cahalan, 1985; Deutsch, Krause, and Lee, 1986). The discovery of swelling-activated Cl^- channels in lymphocytes suggested a possible Ca^{2+}-independent mechanism for RVD (Cahalan and Lewis, 1988; Lewis, Ross, and Cahalan, 1993), in which the opening of Cl^- channels during cell swelling would trigger the loss of Cl^- ions and membrane depolarization. Depolarization in turn would activate K_V channels leading to increased loss of K^+ ions along with osmotically obligated water. More potent K^+-channel blockers and sensitive intracellular Ca^{2+} probes led Grinstein and Smith (1990) to reexamine Ca^{2+}-dependent RVD in T lymphocytes. Charybdotoxin (CTX) potently blocks type *n* K_V channels (Sands, Lewis, and Cahalan, 1989; Price, Lee, and Deutsch, 1989), as well as voltage-independent K_{Ca} channels in HPB T lymphocytes (Grissmer, Nguyen, and Cahalan, 1993). No change in $[Ca^{2+}]_i$ was seen during swelling using the Ca^{2+} indicator indo-1, and CTX inhibited 75% of the RVD response in lymphocytes. Thus, Grinstein and Smith (1990) reasoned that Ca^{2+}-independent, CTX-sensitive and -insensitive K^+ channels govern RVD in HPB T lymphocytes. Therefore, the Ca^{2+}-independent, CTX-sensitive fraction of RVD in HPB T lymphocytes can be attributed to type *n* K_V channels. These channels are encoded by the $K_V1.3$ gene (Doug5 lass, Osborne, Cai, Wilkinson, Christie, and Adelman, 1990; Grissmer, Dethlefs, Wasmuth, Goldin, Gutman, Cahalan, and Chandy, 1992). Recently, transfection of the $K_V1.3$ gene into RVD-incompetent CTLL-2 lymphocytes and subsequent expression of *n*-type K_V channels conferred the ability of these cells to volume regulate, providing further evidence that K_V channels can mediate Ca^{2+}-independent RVD (Deutsch and Chen, 1993).

The data presented in Fig. 15 also indicate that mature mouse thymocytes and HPB lymphocytes rely upon Ca^{2+}-independent RVD during periods of swelling. The absence of SWAC transients in these cells supports this conclusion. Nevertheless, small swelling-induced $[Ca^{2+}]_i$ responses have recently been reported in fluo-3-loaded HPB T cells (Schlichter and Sakellaropoulos, 1994), where it is speculated that Ca^{2+}-dependent and -independent RVD cooperate to control volume. The swelling-induced $[Ca^{2+}]_i$ rise measured by Schlichter and Sakellaropoulos (1994) represents a 36 nM (22°C) to 65 nM (37°C) average $[Ca^{2+}]_i$ rise above resting levels in swollen HPB T lymphocytes. Our fura-2 measurements on swollen HPB T cells and mature mouse thymocytes also suggest a small $[Ca^{2+}]_i$ rise of 40 and 65 nM, respectively (Fig. 15). However, a rise of this magnitude can be produced artifactually by a 10% decrease in the K_d for Ca^{2+} binding to fura-2 as cells swell (Fig. 15 legend). Such a change would be consistent with the difference in fura-2 K_d for Ca^{2+} inside cells as compared with saline solution (reviewed in Negulescu and Machen, 1990). More work is necessary before the effects of small, swelling-induced, $[Ca^{2+}]_i$ changes on RVD can be resolved.

Does a rise in Ca^{2+} play a role in volume regulation by mouse thymocytes? On average, 77% of thymocytes showed SWAC transients that elevated $[Ca^{2+}]_i$ to an average of 650 nM. Data in Fig. 2 illustrate that large deviations in $[Ca^{2+}]_i$ were temporally correlated with an increased rate of RVD in single cells. Cells not exhibiting SWAC transients were also able to volume regulate, but at a slower rate than cells that generated a SWAC transient. The level of $[Ca^{2+}]_i$ achieved during the SWAC

transient would be high enough to activate K_{Ca} channels described previously in activated HPB T cells (Grissmer et al., 1993). Similar CTX-sensitive K_{Ca} channels have been observed in rat and mouse thymocytes (Mahaut-Smith and Mason, 1991; Nguyen and Cahalan, unpublished observation). The activation of K_{Ca} channels during RVD would hyperpolarize the membrane and increase the driving force for efflux of Cl^- ions, as well as providing an optional pathway for K^+ loss. A Ca^{2+}-dependent component of RVD might enable immature mouse thymocytes to shrink rapidly rather than lysing.

Membrane potential (V_m) control and the mechanism of RVD may be different in rat thymocytes. Compared with HPB T cells, rat thymocytes responded somewhat differently to CTX (Grinstein and Smith, 1989). For example, CTX had no effect on the resting V_m, while CTX blocked ionophore-induced, K^+-dependent hyperpolarization in rat thymocytes. Furthermore, CTX did not affect RVD in swollen rat thymocytes. These results led Grinstein and Smith (1990) to conclude that Ca^{2+}-dependent, CTX-sensitive K^+ channels, although present in these cells, did not participate in V_m control or function during RVD. Rather, Ca^{2+}-independent, CTX-insensitive K^+ channels exclusively controlled V_m and contributed to RVD in rat thymocytes. The identity of the Ca^{2+} independent, CTX-insensitive K^+ conductance is uncertain. A CTX-insensitive K_V current has been identified in HPB T lymphocytes (Lee, Levy, and Deutsch, 1992), but its possible role in mediating CTX-insensitive RVD in rat thymocytes and HPB T lymphocytes has not been examined.

A Physiological Role for SWAC Transients

SWAC transients in immature mouse thymocytes may indicate that volume control is critical during early stages of lymphocyte development. It is possible that mouse thymocytes switch from Ca^{2+}-dependent to Ca^{2+}-independent RVD as they mature. However, enhanced RVD in immature T cells is not a universal phenomenon. Grinstein and Smith (1990) have reported that rat thymocytes, albeit a mixture of mature and immature phenotypes, do not return to control volume as quickly as HPB T lymphocytes. An alternative consideration is that $[Ca^{2+}]_i$ transients, although activated by swelling, may be related to other functions in immature mouse thymocytes besides volume regulation.

Intrathymic T-cell development and selection processes require close interaction between thymocytes and the surrounding microenvironment (Scollay, Wilson, D'Amico, Kelly, Egerton, Pearse, Wu, and Shortman, 1988; Ritter and Boyd, 1993). As thymocytes mature, they migrate within the thymus from the cortical subcapsular region to the central medulla. Signals for clonal proliferation, receptor gene rearrangement, positive selection of appropriate MHC interactions, negative selection of self reactive and defective cells, are delivered to thymocytes throughout development. The thymic microenvironment supplies these signals via stromal cells (fibroblasts, epithelial cells, dendritic cells, macrophages, et cetera), which closely interact with developing thymocytes. A rise in $[Ca^{2+}]_i$ is believed to mediate the clonal deletion of immature, self-reactive, $CD4^+CD8^+$ thymocytes by apoptosis (McConkey, Jondal, and Orrenius, 1994). Thymocyte apoptosis can be stimulated by Ca^{2+} ionophores and anti-TCR antibodies. If SWAC transients can be elicited by membrane stretch during adhesive interactions between stromal cells and thymocytes, they may contribute to Ca^{2+}-mediated apoptosis in vivo.

We thank Drs. Miriam Ashley-Ross and Paul Negulescu for extended discussions throughout this project. Dr. Rich Lewis and Ms. Ruth Davis provided critical comments on the manuscript.

Supported by a Biotechnology Corporate Affiliated Graduate Student Fellowship to P. E. Ross and NIH grants NS14609 and GM41514 to M. D. Cahalan.

Original version received 23 November 1994 and accepted version received 27 March 1995.

REFERENCES

Berridge, M. J. 1993. Inositol trisphosphate and calcium signalling. *Nature.* 361:315–325.

Botchkin, L. M., and G. Matthews. 1993. Cell volume changes are accompanied by artifactual changes in internal calcium as measured by fura-2 fluorescence. *Biophysical Journal.* 64:A78. (Abstr.)

Bui, A. H., and J. S. Wiley. 1981. Cation fluxes and volume regulation by human lymphocytes. *Journal of Cellular Physiology.* 108:47–54.

Cahalan, M. D., and R. S. Lewis. 1988. Role of potassium and chloride channels in volume regulation by T lymphocytes. *In* Cell Physiology of Blood. R. B. Gunn and J. C. Parker, editors. Rockefeller University Press, New York. 281–301.

Carafoli, E. 1991. Calcium pump of the plasma membrane. *Physiological Reviews.* 71:129–153.

Cheung, R. K., S. Grinstein, H.-M. Dosch, and E. W. Gelfand. 1982*a*. Volume regulation by human lymphocytes: characterization of the ionic basis for regulatory volume decrease. *Journal of Cellular Physiology.* 112:189–196.

Cheung, R. K., S. Grinstein, and E. W. Gelfand. 1982*b*. Volume regulation by human lymphocytes. Identification of differences between the two major lymphocyte subpopulations. *Journal of Clinical Investigation.* 70:632–638.

Crabtree, G. R., and N. A. Clipstone. 1994. Signal transmission between the plasma membrane and nucleus of T lymphocytes. *Annual Review of Biochemistry.* 63:1045–1083.

DeCoursey, T. E., K. G. Chandy, S. Gupta, and M. D. Cahalan. 1985. Voltage-dependent ion channels in T-lymphocytes. *Journal of Neuroimmunology.* 10:71–95.

Demaurex, N., D. P. Lew, and K.-H. Krause. 1992. Cyclopiazonic acid depletes intracellular Ca^{2+} stores and activates an influx pathway for divalent cations in HL-60 cells. *Journal of Biological Chemistry.* 267:2318–2324.

Densmore, J. J., G. Szabo, and L. S. Gray. 1992. A voltage-gated calcium channel is linked to the antigen receptor in Jurkat T lymphocytes. *FEBS Letters.* 312:161–164.

Deutsch, C., and L.-Q. Chen. 1993. Heterologous expression of specific K^+ channels in T lymphocytes: functional consequences for volume regulation. *Proceedings of the National Academy of Sciences, USA.* 90:10036–10040.

Deutsch, C., D. Krause, and S. C. Lee. 1986. Voltage-gated potassium conductance in human T lymphocytes stimulated with phorbol ester. *Journal of Physiology.* 372:405–423.

Deutsch, C., and S. C. Lee. 1988. Cell volume regulation in lymphocytes. *Renal Physiology and Biochemistry.* 3–5:260–276.

Dolmetsch, R. E., and R. S. Lewis. 1994. Signaling between intracellular Ca^{2+} stores and depletion-activated Ca^{2+} channels generates $[Ca^{2+}]_i$ oscillations in T lymphocytes. *Journal of General Physiology.* 103:365–388.

Douglass, J., P. B. Osborne, Y. C. Cai, M. Wilkinson, M. J. Christie, and J. P. Adelman. 1990. Characterization and functional expression of a rat genomic DNA clone encoding a lymphocyte potassium channel. *Journal of Immunology.* 144:4841–4850.

Dupuis, G., J. Héroux, and M. D. Payet. 1989. Characterization of Ca^{2+} and K^+ currents in the human Jurkat T cell line: effects of phytohaemagglutinin. *Journal of Physiology.* 412:135–154.

Foskett, J. K. 1988. Simultaneous Nomarski and fluorescence imaging during video microscopy of cells. *American Journal of Physiology.* 255:C566–C571.

Gouy, H., D. Cefai, S. B. Christensen, P. Debré, and G. Bismuth. 1990. Ca^{2+} influx in human T lymphocytes is induced independently of inositol phosphate production by mobilization of intracellular Ca^{2+} stores. A study with the Ca^{2+} endoplasmic reticulum-ATPase inhibitor thapsigargin. *European Journal of Immunology.* 20:2269–2275.

Grinstein, S., S. Cohen, B. Sarkadi, and A. Rothstein. 1983. Induction of ^{86}Rb fluxes by Ca^{2+} and volume changes in thymocytes and their isolated membranes. *Journal of Cellular Physiology.* 116:352–362.

Grinstein, S., A. Dupre, and A. Rothstein. 1982. Volume regulation by human lymphocytes: role of calcium. *Journal of General Physiology.* 79:849–868.

Grinstein, S., A. Rothstein, B. Sarkadi, and E. W. Gelfand. 1984. Responses of lymphocytes to anisotonic media: volume-regulating behavior. *American Journal of Physiology.* 246:C204–C215.

Grinstein, S., and J. D. Smith. 1989. Ca^{2+} induces charybdotoxin-sensitive membrane potential changes in rat lymphocytes. *American Journal of Physiology.* 257:C197–C206.

Grinstein, S., and J. D. Smith. 1990. Calcium-independent cell volume regulation in human lymphocytes. Inhibition by charybdotoxin. *Journal of General Physiology.* 95:97–120.

Grissmer, S., B. Dethlefs, J. Wasmuth, A. L. Goldin, G. A. Gutman, M. D. Cahalan, and K. G. Chandy. 1990. Expression and chromosomal localization of a lymphocyte K^+ channel gene. *Proceedings of the National Academy of Sciences, USA.* 87:9411–9415.

Grissmer, S., A. N. Nguyen, and M. D. Cahalan. 1993. Calcium-activated potassium channels in resting and activated human T lymphocytes. *Journal of General Physiology.* 102:601–630.

Grynkiewicz, G., M. Poenie, and R. Y. Tsien. 1985. A new generation of Ca^{2+} indicators with greatly improved fluorescence properties. *Journal of Biological Chemistry.* 260:3440–3450.

Hess, S. D., M. Oortgiesen, and M. D. Cahalan. 1993. Calcium oscillations in human T and natural killer cells depend upon membrane potential and calcium influx. *Journal of Immunology.* 150:2620–2633.

Hille, B. 1992. Ionic Channels of Excitable Membranes. Second edition. Sinauer Associates, Inc., Sunderland, MA. 108–111.

Hoffmann, E. K., L. O. Simonsen, and I. H. Lambert. 1993. Cell volume regulation: intracellular transmission. *In* Advances in Comparative and Environmental Physiology. Vol. 14. F. Lang and D. Häussinger, editors. Springer-Verlag, Berlin. 187–248.

Hoth, M., and R. Penner. 1992. Depletion of intracellular calcium stores activates a calcium current in mast cells. *Nature.* 355:353–356.

Hoth, M., and R. Penner. 1993. Calcium release-activated calcium current in rat mast cells. *Journal of Physiology.* 465:359–386.

Khan, A. A., J. P. Steiner, M. G. Klein, M. F. Schneider, and S. H. Snyder. 1992. IP_3 receptor: localization to plasma membrane of T cells and cocapping with the T cell receptor. *Science.* 257:815–818.

Kuno, M., and P. Gardner. 1987. Ion channels activated by inositol 1,4,5-triphosphate in plasma membrane of human T-lymphocytes. *Nature.* 326:301–304.

Kuno, M., J. Goronzy, C. M. Weyand, and P. Gardner. 1986. Single-channel and whole-cell recordings of mitogen-regulated inward currents in human cloned helper T lymphocytes. *Nature.* 323:269–273.

Kwan, C. Y., H. Takemura, J. F. Obie, O. Thastrup, and J. W. Putney, Jr. 1990. Effects of MeCh, thapsigargin, and La^{3+} on plasmalemmal and intracellular Ca^{2+} transport in lacrimal acinar cells. *American Journal of Physiology.* 258:C1006–C1015.

Lee, S.C., D. I. Levy, and C. Deutsch. 1992. Diverse K^+ channels in primary human T lymphocytes. *Journal of General Physiology.* 99:771–793.

Lewis, R. S., and M. D. Cahalan. 1989. Mitogen-induced oscillations of cytosolic Ca^{2+} and transmembrane Ca^{2+} current in human leukemic T cells. *Cell Regulation.* 1:99–112.

Lewis, R. S., and M. D. Cahalan. 1995. Potassium and calcium channels in lymphocytes. *Annual Review of Immunology.* 13:623–653.

Lewis, R. S., P. E. Ross, and M. D. Cahalan. 1993. Chloride channels activated by osmotic stress in T lymphocytes. *Journal of General Physiology.* 101:801–826.

Lückhoff, A., and D. E. Clapham. 1994. Calcium channels activated by depletion of internal calcium stores in A431 cells. *Biophysical Journal.* 67:177–182.

Mahaut-Smith, M. P., and M. J. Mason. 1991. Ca^{2+}-activated K^+ channels in rat thymic lymphocytes: activation by concanavalin A. *Journal of Physiology.* 439:513–528.

Mason, M. J., C. Garcia-Rodriguez, and S. Grinstein. 1991*a*. Coupling between intracellular Ca^{2+} stores and the Ca^{2+} permeability of the plasma membrane. *Journal of Biological Chemistry.* 266: 20856–20862.

Mason, M. J., M. P. Mahaut-Smith, and S. Grinstein. 1991*b*. The role of intracellular Ca^{2+} in the regulation of the plasma membrane Ca^{2+} permeability of unstimulated rat lymphocytes. *Journal of Biological Chemistry.* 266:10872–10879.

McCarty, N. A., and R. G. O'Neil. 1992. Calcium signaling in cell volume regulation. *Physiological Reviews.* 72:1037–1061.

McConkey, D. J., M. Jondal, and S. Orrenius. 1994. The regulation of apoptosis in thymocytes. *Biochemical Society Transactions.* 22:606–610.

Montero, M., J. Alvarez, and J. Garcia-Sancho. 1990. Uptake of Ca^{2+} and refilling of intracellular Ca^{2+} stores in Ehrlich-ascites-tumour cells and in rat thymocytes. *Biochemical Journal.* 271:535–540.

Morris, C. E. 1990. Mechanosensitive ion channels. *Journal of Membrane Biology.* 113:93–107.

Negulescu, P. A., and T. E. Machen. 1990. Intracellular ion activities and membrane transport in parietal cells measured with fluorescent dyes. *Methods in Enzymology.* 192:38–81.

Negulescu, P. A., N. Shastri, and M. D. Cahalan. 1994. Intracellular calcium dependence of gene expression in single T lymphocytes. *Proceedings of the National Academy of Sciences, USA.* 91:2873–2877.

Premack, B. A., T. V. McDonald, and P. Gardner. 1994. Activation of Ca^{2+} current in Jurkat T cells following the depletion of Ca^{2+} stores by microsomal Ca^{2+}-ATPase inhibitors. *Journal of Immunology.* 152:5226–5240.

Price, M., S. C. Lee, and C. Deutsch. 1989. Charybdotoxin inhibits proliferation and interleukin 2 production in human peripheral blood lymphocytes. *Proceedings of the National Academy of Sciences, USA.* 86:10171–10175.

Putney, J. W. 1990. Capacitative calcium entry revisited. *Cell Calcium.* 11:611–624.

Rink, T. J., A. Sanchez, S. Grinstein, and A. Rothstein. 1983. Volume restoration in osmotically swollen lymphocytes does not involve changes in free Ca^{2+} concentration. *Biochimica et Biophysica Acta.* 4:115–135.

Ritter, M. A., and R. L. Boyd. 1993. Development in the thymus: it takes two to tango. *Immunology Today.* 14:462–469.

Ross, P. E. 1991. Hypoosmotic stress generates calcium transients in mouse thymocytes. *Biophysical Journal.* 59:598*a*. (Abstr.)

Ross, P. E., and M. D. Cahalan. 1995. Swelling- and depletion-activated Ca^{2+} influx pathways in mouse thymocytes. *Biophysical Journal.* 68:A55. (Abstr.)

Ross, P. E., S. S. Garber, and M. D. Cahalan. 1994. Membrane chloride conductance and capacitance in Jurkat T lymphocytes during osmotic swelling. *Biophysical Journal.* 66:169–178.

Rotin, D., M. J. Mason, and S. Grinstein. 1991. Channels, antiports, and the regulation of cell volume in lymphoid cells. *In* Advances in Comparative and Environmental Physiology, Vol. 9. R. Gilles, E. K. Hoffmann, and L. Bolis, editors. Springer-Verlag, Berlin. 187–248.

Sands, S. B., R. S. Lewis, and M. D. Cahalan. 1989. Charybdotoxin blocks voltage-gated K^+channels in human and murine T lymphocytes. *Journal of General Physiology.* 93:1061–1074.

Sarkadi, B., A. Tordai, L. Homolya, O. Scharff, and G. Gardos. 1991. Calcium influx and intracellular calcium release in anti-CD3 antibody-stimulated and thapsigargin-treated human T lymphoblasts. *Journal of Membrane Biology.* 123:9–21.

Scharff, O., and B. Foder. 1993. Regulation of cytosolic calcium in blood cells. *Physiological Reviews.* 73:547–582.

Schlichter, L. C., and G. Sakellaropoulos. 1994. Intracellular Ca^{2+} signaling induced by osmotic shock in human T lymphocytes. *Experimental Cell Research.* 215:211–222.

Scollay, R., A. Wilson, A. D'Amico, K. Kelly, M. Egerton, M. Pearse, L. Wu, and K. Shortman. 1988. Developmental status and reconstitution potential of subpopulations of murine thymocytes. *Immunological Reviews.* 104:81–120.

Thastrup, O., A. P. Dawson, O. Scharff, B. Foder, P. J. Cullen, B. K. Drøbak, P. J. Bjerrum, S. B. Christensen, and M. R. Hanley. 1989. Thapsigargin, a novel molecular probe for studying intracellular calcium release and storage. *Agents and Actions.* 27:17–23.

Tsien, R. W., and R. Y. Tsien. 1990. Calcium channels, stores, and oscillations. *Annual Review of Cell Biology.* 6:715–760.

Zweifach, A., and R. S. Lewis. 1993. Mitogen-regulated Ca^{2+} current of T lymphocytes is activated by depletion of intracellular Ca^{2+} stores. *Proceedings of the National Academy of Sciences, USA.* 90:6295–6299.